USAARL Report No. 87-1

HEAD MOVEMENTS DURING CONTOUR FLIGHT

By

Robert W. Verona

Clarence E. Rash

William R. Holt

John K. Crosley

SENSORY RESEARCH DIVISION
RESEARCH SYSTEMS DIVISION

October 1986

Approved for public release, distribuUon unlimited.

Notice

Qualified requesters

Qualified requesters may obtain copies from the Defense Technical Information Center (DTIC), Cameron Station, Alexandria, Virginia 22314. Orders will be expedited if placed through the librarian or other person designated to request documents from DTIC.

Change of address

Organizations receiving reports from the US Army Aeromedical Research Laboratory on automatic mailing lists should confirm correct address when corresponding about laboratory reports.

Disposition

Destroy this document when it is no longer needed. Do not return it to the originator.

Disclaimer

The views, opinions, and/or findings contained in this report are those of the author(s) and should not be construed as an official Department of the Army position, policy, or decision, unless so designated by other official documentation. Citation of trade names in this report does not constitute an official Department of the Army endorsement or approval of the use of such commercial items.

Reviewed:

Bruce C. Leibrecht

BRUCE C. LEIBRECHT, Ph.D.
LTC, MS
Director, Sensory Research Division

Released for publication:

J. D. LaMothe

J. D. LaMOTHE, PH.D.
COL, MS
Chairman, Scientific
Review Committee

Dudley R. Price

DUDLEY R. PRICE
Colonel, MC
Commanding

UNCLASSIFIED

SECURITY CLASSIFICATION OF THIS PAGE (When Data Entered)

REPORT DOCUMENTATION PAGE		READ INSTRUCTIONS BEFORE COMPLETING FORM
1. REPORT NUMBER USAARL Report No. 87-1	2. GOVT ACCESSION NO.	3. RECIPIENT'S CATALOG NUMBER
4. TITLE (and Subtitle) Head Movements During Contour Flight		5. TYPE OF REPORT & PERIOD COVERED Final Report 6. PERFORMING ORG. REPORT NUMBER
7. AUTHOR(s) Robert W. Verona, Clarence E. Rash, William R. Holt, and John K. Crosley		8. CONTRACT OR GRANT NUMBER(s)
9. PERFORMING ORGANIZATION NAME AND ADDRESS US Army Aeromedical Research Laboratory Fort Rucker, AL 36362-5292		10. PROGRAM ELEMENT, PROJECT, TASK AREA & WORK UNIT NUMBERS 64207.A,4E4642070425, 00,048
11. CONTROLLING OFFICE NAME AND ADDRESS		12. REPORT DATE October 1986 13. NUMBER OF PAGES 78
14. MONITORING AGENCY NAME & ADDRESS(if different from Controlling Office) US Army Medical Research and Development Command Fort Detrick Frederick, MD 21701-5012		15. SECURITY CLASS. (of this report) UNCLASSIFIED 15a. DECLASSIFICATION/DOWNGRADING SCHEDULE
16. DISTRIBUTION STATEMENT (of this Report) Distribution unlimited.		
17. DISTRIBUTION STATEMENT (of the abstract entered in Block 20, if different from Report)		
18. SUPPLEMENTARY NOTES		
19. KEY WORDS (Continue on reverse side if necessary and identify by block number) head tracking contour flight head velocity visually coupled system (VCS)		
20. ABSTRACT (Continue on reverse side if necessary and identify by block number) See reverse		

DD FORM 1 JAN 73 1473 EDITION OF 1 NOV 65 IS OBSOLETE

UNCLASSIFIED

SECURITY CLASSIFICATION OF THIS PAGE (When Data Entered)

20. ABSTRACT

This head movement study was conducted to measure pilot head rotational movements during contour flights. The head movement data were collected from five subjects as each flew a modified UH-1M over a 15-mile contour course. The subject pilots also were required to visually search for an "enemy" aircraft while flying the contour course. A helmet-mounted sight was used to measure the pilots' head movements. The head position data indicate the pilots looked forward most of the time, even though the scenario required a broad range of head movements. The data also suggest pure head-neck movements without torso participation. The head velocity data indicate symmetrical azimuth and elevation head movement components. Approximately 97 percent of the head movements were equal to or less than 120E/sec, although some movements exceeded 200O/sec.

LTC Robert W. Verona currently is assigned to the Night Vision and Electro-Optics Laboratory, Fort Belvoir, VA.

Table of contents

List of figures

List of Tables

INTRODUCTION

Aircraft and weapon systems engineers are interested in learning more about a pilot's head movements during flying missions. These engineers are using the pilot's head as a control device. As they learn more about a pilot's natural head movements, they can more effectively use his head as a controller.

When a pilot's head position is used as a control input, his head/helmet position is tracked, and the tracking information is used to slave a gimballed platform. The pilot can aim a day/night television camera, for example, or a weapon mounted on the platform just by moving his head. A very small television display attached to the pilot's helmet provides feedback from the TV camera to the pilot so he can see where he is aiming. While watching a virtual image video display, the pilot fine tunes his aim with small head movements and places his display's crosshairs on the target.

This type of control system is called a Visually Coupled System (VCS). It is a closed-loop servo-system using the natural visual and motor skills of the pilot to remotely control a weapon and/or sensor. The Army's Advanced Attack Helicopter, the Apache, has this system.

System engineers easily can compromise a pilot's performance if their VCS design is not sound. A sound design must be based on solid functional requirements. During the late 1970s, values for some VCS design requirements could not be found in the scientific literature and had to be estimated until empirical evidence could be gathered.

One of the functional requirements missing was a platform maximum movement rate. If the platform is to follow the pilot's head, we must know how fast the pilot turns his head when he is flying. Does he rotate it at the same speed up and down, as he does left and right? These are important VCS parameters since over-specifying them would be costly, and under-specifying them would degrade performance.

Experiences in flight tests conducted with prototype VCS hardware suggested pilots tended to look primarily forward with minimal rapid head motions. However, observations during test flights did not agree with similar observations of pilots flying nontest missions. The experiment described in this paper was designed to obtain realistic pilot head movement data in a demanding flight scenario. These data also would support or question the 120E/sec head movement rate estimate used to design the Apache's VCS systems.

BACKGROUND

Medical specialists have studied head movements in their laboratories. They report that normal adults can rotate their heads +/-90° in azimuth with neck participation, and-100 to +25° in elevation without neck participation {Allen and Webb, 1983). The head rotational velocities observed during Allen's and Webb's experiment were compared to published biomechanical data. The published peak head velocity and acceleration data show there is a functional dependence on motion range. The peak velocity and acceleration for a 5° head movement are 48°/sec and 551°/sec^{2,} reSPectively. The pea~ velociy ana acceleration for a 60 head movement are 3520/sec and 3,300u/ sec^{2,} respectively. The time for the movements did notchange significantly, but the velocity and the accelerations did. A six-fold increase in the velocity and acceleration accompanied a 5° to 60° range of motion change (Zangemeister and Stark, 1981).

Very few studies have been published containing biomechanical data on head movements collected in an actual or simulated aircraft environment. Whole body vibration (Verona, Johnson, and Jones, 1979; Johnson, Priser, and Verona, 1981} and the addition of a flight helmet {Phillips and Petrofsky, 1983), significant factors in an aircraft's environment, would reduce peak movement parameter values from man's measured maximum capabilities.

METHODOLOGY

AIRCRAFT

Two rotary-wing aircraft were used in the study, a modified utility helicopter, JUH-1M, and an observation helicopter, JOH-58. The subject pilot, a safety pilot, an experimenter, and a technician flew in the instrumented JUH-1M test aircraft. The JOH-58 served two functions: first, it was the normal chase/safety aircraft; second, it assumed the mission of the thr^{eat} aircraft discussed in the procedure section.

INSTRUMENTATION

The JUH-1M was equipped with a slewable television camera, prototype vCS hardware, and a data acquisiti^{En} instrumentation package. Th~ teleViSion camera was used to document the test flights. The VCS hardware, provided by Honeywell, Inc.,* included a helmet-mounted sighting system {HMS), a helnmt-mounted display (HMD), and a prototype helmet which integrated the head-supported components.

* See Appendix C

The HMS tracked the position of the pilot's head/helmet. It provided coverage of +/-180o azimuth and +30o/-90º elevation with half a degree accuracy. A boresight reticle unit, part of the HMS, provided a collimated sighting reference point inside the aircraft.

The HMD generated an illuminated crosshair on a transparent monocle in front of the pilot's right eye. The HMD was only used to calibrate the pilot's line-of-sight; it was removed for the test flights.

A prototype of the helmet for use in the Apache was electronically adapted for the JUH-1M. The helmet served as a mounting platform for the HMS detectors and the HMD, as well as for the normal communications headset and microphone.

The HMS measured the head/helmet position every 40 ms during the test flights. These position data were multiplexed with aircraft data and recorded. The aircraft data recorded were heading, altitude, attitude, airspeed, and aircraft ground track. The video from the TV camera, which was slaved to the pilot's head movements, and audio from the aircraft's intercom and radios also were recorded. All of the experimental data were recorded on 30-minute video cassettes. Each trial lasted about 25 minutes and was recorded on a separate cassette.

SUBJECTS

Six male US Army aviators served as volunteer subjects. All were qualified in the UH-1M helicopter and were stationed at Fort Rucker, Alabama, in flying assignments. Subject #4 was a medevac pilot with previous search and rescue experience.

SAFETY

A safety pilot sat in the right seat of the JUH-1M during all test flights. He was familiar with the extensive JUH-1Mmodifications and discussed them with each subject before the test flight. The safety pilot also designed and monitored the flight course. He navigated for the subjects on their first pass through the course and checked the subject pilot's navigation on the second pass. Observers in the chase aircraft continuously monitored the test aircraft.

PROCEDURES

All of the test data were collected on the same day. Four subjects were tested in the morning and two in the afternoon. The subjects were flown to the test area two-at-a-time and were segregated un~il the final debriefing. Each subject was briefed individually before his test flights. They were not told their head movements were the focus of this experiment until after th~-study. They were told they would be wearing a prototype helmet and the experimenters were interested in their opinion of the helmet.

The subjects also were instructed to look for a threat aircraft. This aircraft would appear somewhere in their field-of-view during the flight. They were to use the intercom to alert the safety pilot when they saw it.

After the briefing, the life-support equipment specialist fitted the prototype helmet to the subject and led him to the test aircraft. The subject pilot sat in the left seat and the safety pilot sat in the right seat. The HMD was attached to the helmet and the boresight procedure was executed. The subject lined up the crosshair generated on the transparent HMD with the boresight reticle unit's crosshair. The subject signalled when the cross-hairs were lined up and the HMS computer recorded his helmet position. This helmet position corresponded to a OO azimuth and -10o elevation line-of-sight. The HMD then was removed and stowed. If the subject removed his helmet, this boresight procedure was repeated.

The safety pilot then started the aircraft and briefed the subject pilot on the aircraft's unique handling qualities. The subject took the controls and maneuvered the aircraft in the remote heliport area until he felt comfortable enough to begin the first trial. The safety pilot navigated throughout the first trial as the subject pilot flew the aircraft. The subject pilot performed his own navigation on the second trial. Each flight lasted about 25 minutes, with an average ground speed near 50 knots. The altitude range during the flights was 10 to 150 feet above ground level.

The chase/threat pilot was directed to position his aircraft in the subject pilot's field-of-view a minimum of three times during each trial. As a safety precaution, the chase pilot transmitted his intentions to the safety pilot using a radio the subject could not monitor.

The course was circular so both aircraft returned to the heliport at the end of each trial. After the first trial, the subject pilot was given an opportunity to land and rest a few minutes before his second trial. A new data tape was inserted and the boresight was checked. At the conclusion of the second trial, the aircraft was shut down and the subject was debriefed.

RESULTS

The independent variable in this study was time and the dependent variables were head rotational position and head rotational velocity. Head translation, whether side to side, fore and aft, or up and down, was not measured. The dependent variable data were collected as a time series of line-of-sight vectors. During each 25-minute flight, the HMS computer generated 240,000 line-of-sight data samplesi the first and last few minutes of each flight's data were not processed. The data from subject #2 were not incorporated into the following analyses due to loss of boresight; the collected data indicated equipment failure and were therefore rejected.

The HMS data were analyzed and viewed from three different perspectives. First, the line-of-sight vectors were mathematically converted to azimuth data and elevation data and then analyzed independently. Histograms developed from the azimuth data and elevation data show the frequency distribution as a function of head azimuth or elevation angle (Figures 1 and 2). Each frequency cell has a I^{o} width and frequencies were plotted as a function of the cell's midpoint.

In the second analysis, velocity calculations were made from the time-sequenced azimuth and elevation position data. The time between data samples was known, so the velocity from one sequential position to another could be calculated. Histograms developed from the azimuth velocity data and elevation velocity data show the frequency distribution as a function of head azimuth or elevation angular velocity (Figures 3 through 6). A frequency cell width of lO/sec was used.

An attempt to generate head acceleration data from the sequential velocity data failed. The acceleration calculations produced unreliable values.

The third analysis was done using the line-of-sight vectors. These data are presented in a unique graphic format (Figures 7 through 12). (Note: Data for subject #2 were graphed also to show they were determined to be invalid.) An outline was made of the test aircraft's windows as seen by the subject

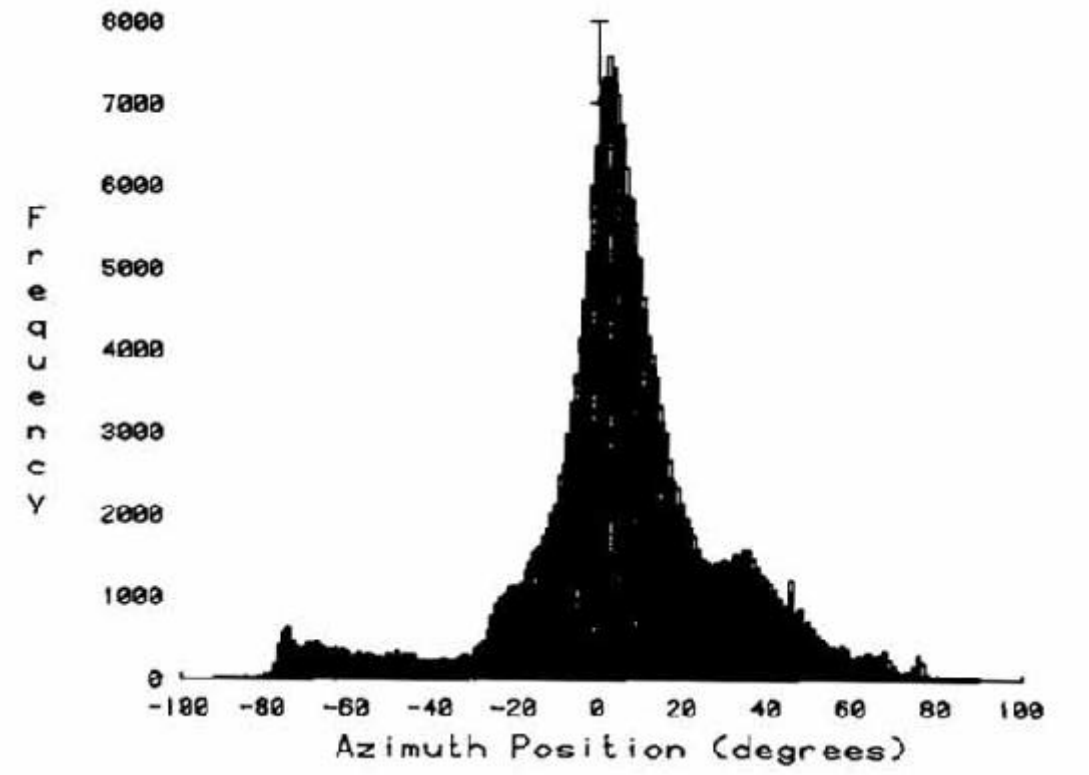

FIGURE 1. Frequency histogram for azimuth position.

pilot. Line-of-sight vectors for the first 4 minutes of analyzed head movement data were plotted on the.window area. Each dot represents at least one line-of-sight measurement sampled at 1-second intervals; some of the dots are overprinted.

The mean, median, standard deviation, skewness, ~nd kurtosis of the approximately 240,000 azimuth and 240,000 elevation head position data values for each trial are presented in Tables 1 and 2, respectively. Similarly, the azimuth and elevation velocity summary statistics are presented in Tables 3 and 4.

The positive means and medians in Table 1 indicate that the pilots were looking slightly right, toward the center of the aircraft, most of the time. (NOte: 0^{o} ~zimuth is directl^{y} i^{n} front of the pilot, not the center of the aircraft.) The large sta~ard deviations in Table ! suggest that the pilots exhibited considerable variability with respect to position while performing the search task.

Figure 1 shows the summation of the azimuth position da~,.exce~t subject #2. The azimuth range is from .goo to +goo. The slight peak at -zb corresponds to the center of the aircraft door window. The major contribution to this p?ak was made by subject #4, the search and rescue (SAR) pilot. The-450 to -30 region is blocked by theairCraft structure. The majo^{r} peak indicates, as above, that the pilots spent most of their time looking right of center.

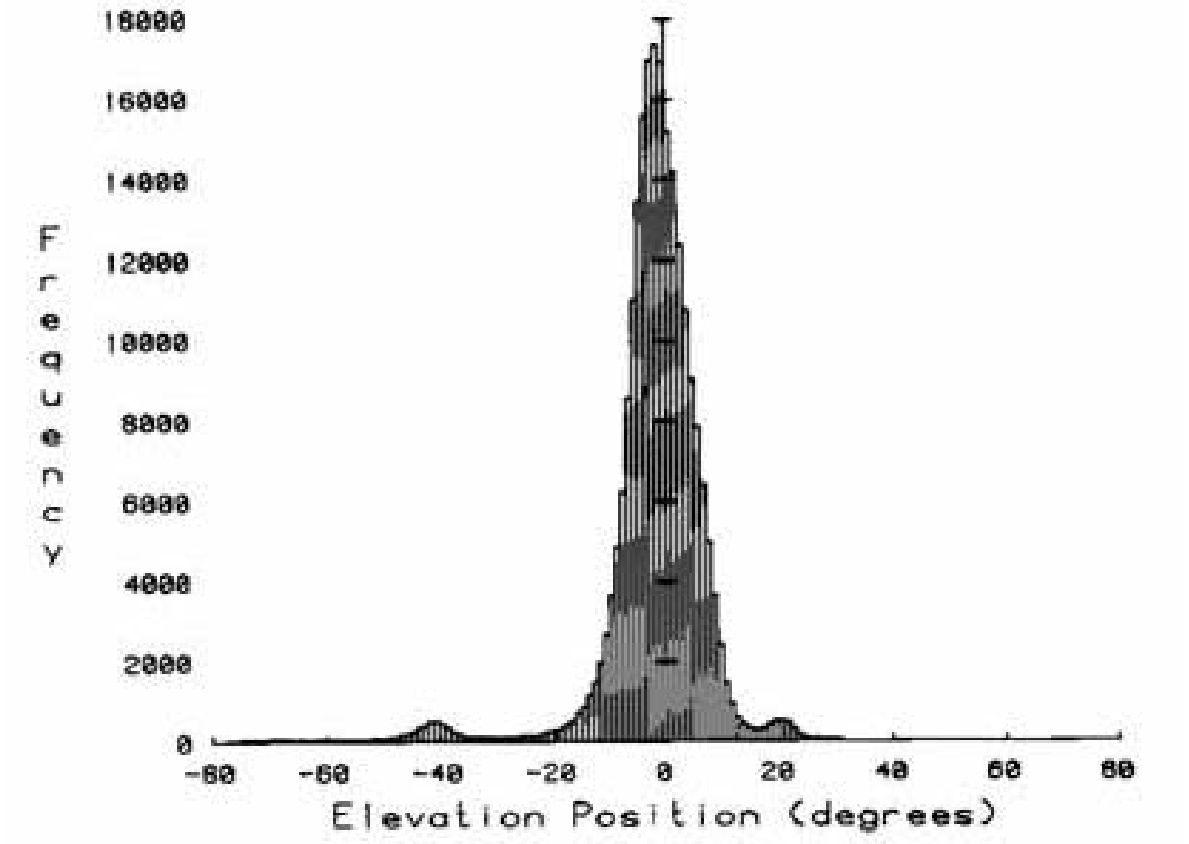

FIGURE 2. Frequency histogram for elevation position.

The elevation position range is from -65o to +30°. The major peak occurs at -lO. Further examining Figure 2, we find a small hump at -40° corresponding to the position of the chin transparency; again, the major contributor to this peak was subject #4. Another small hump centered at +20° is probably the result of the upward search for the threat aircraft. The pilots spent 95 percent of their time looking between -14o and +14o; the pilot's heads remained essentially level.

The standard deviations in Table 2 are not as large as those in Table 1; this suggests elevation movements were not over as large a range as the azimuth movements. The negative elevation medians in Table 2 indicate that the pilots were looking down more often than they were looking up.

The summary statistics for azimuth and elevation angular rates are presented in Tables 3 and 4, respectively. The reliability of the velocity analysis is supported by the clustering of the means, standard deviations, and medians for both within and between subjects. However, the measures of central tendency presented in the summary statistics are not as illustrative of pilot head motion as the range of the rate values. These rate data are shown as angular rate histograms in Figures 3 and 5.

Investigating the azimuth data in Table 3, we find Subject #6 has the largest within-subject variation in the median, 8°/sec. The other subjects

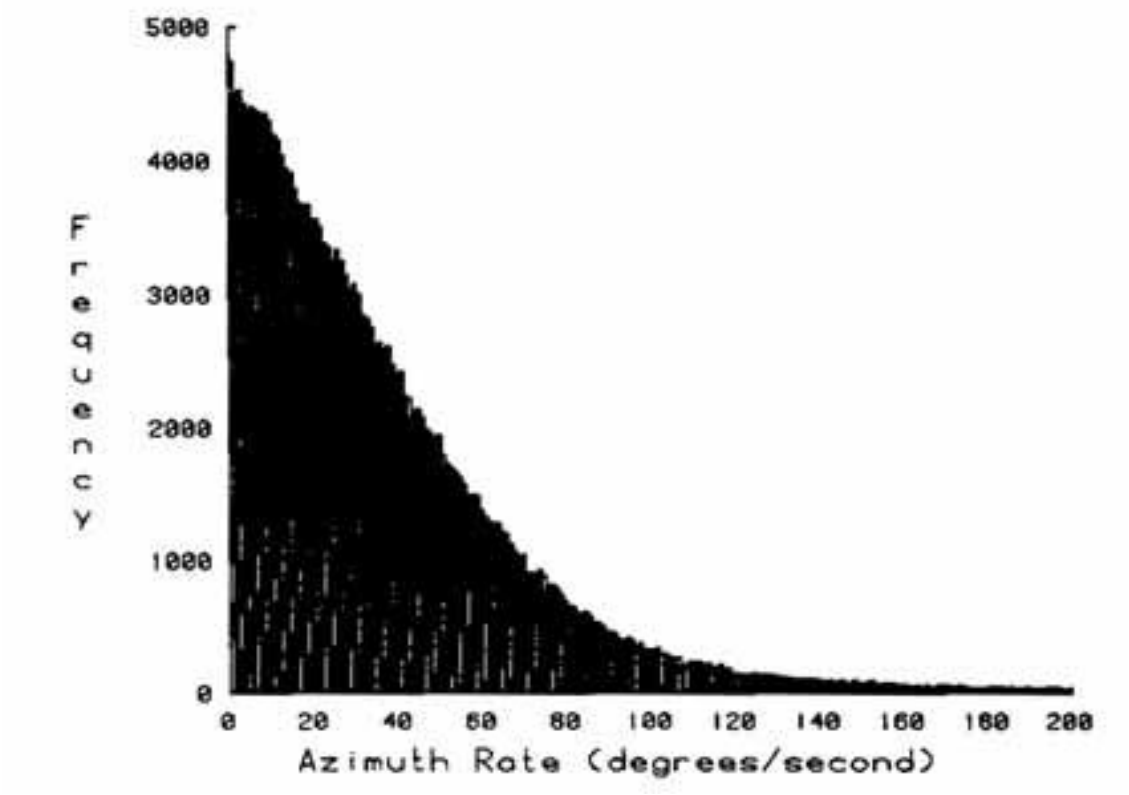

FIGURE 3. Frequency histogram for azimuth velocity.

have within-subject variations of about 3°/sec. The small medians indicate that the velocity distribution is weighted heavily towards the lower value. The variability between subjects is greater than the variability within subjects, underlining the role of individual differences in search dynamics.

There is greater variability in the elevation velocity data (Table 4). The within-subject variability in the median ranges from about 1 to 11 degrees per second and between-subject differences in the median for the subject's combined trials range from approximately 0 to 9 degrees per second. Subject #6 had the largest variability again. The medians, also, were again smaller than the means indicating more data points at the lower angular rates.

The cumulative frequency plots of the angular velocity d~ba (Figures 4 and 6} indicate that 50 percent of the elevation and azimuth rates were less than or equal to 32°/sec. The median data in Tables 3 and 4 also support this statement. The plots also show that go percent of the elevation and azimuth rates were less than or equal to 8O°/sec.

There were more instances Of higher azimuth rates then elevation rates, according to Figures 3 and 5. The relative frequency approaches zero at about

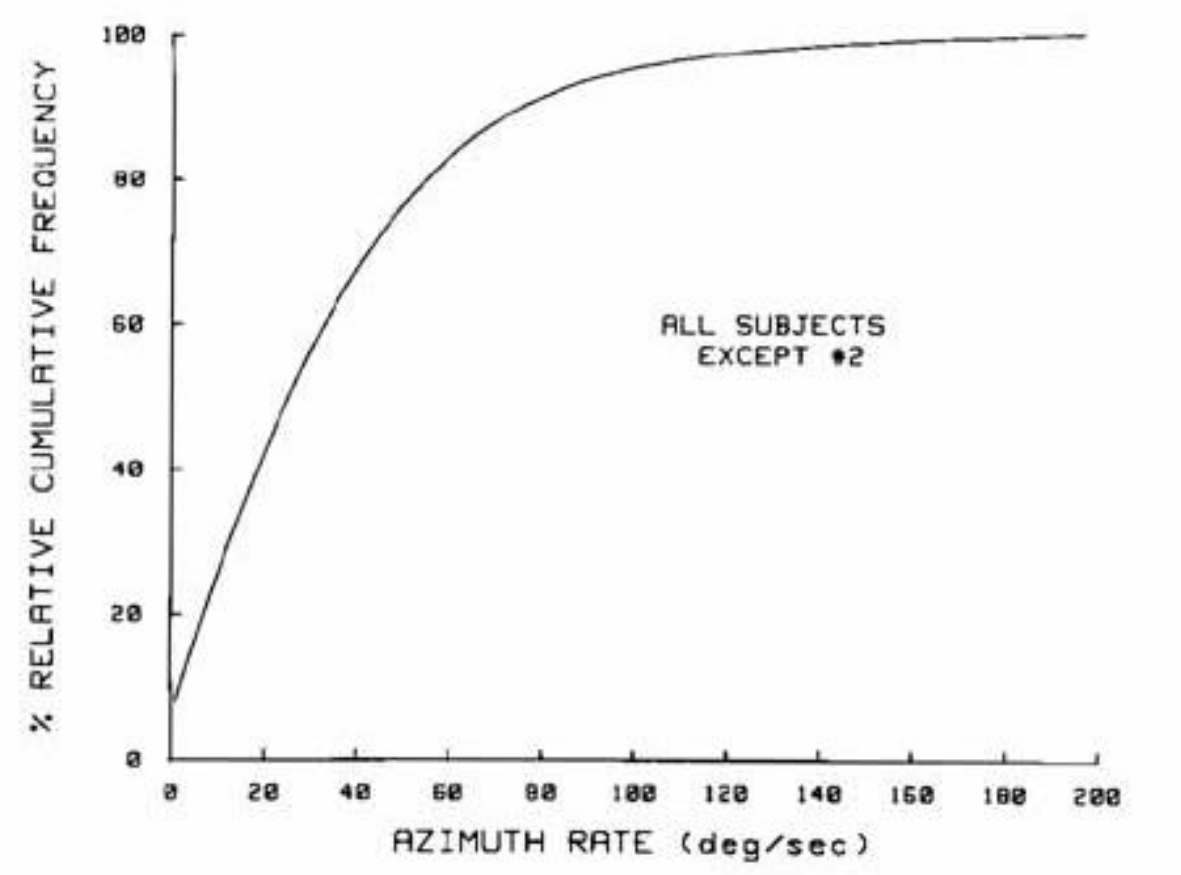

FIGURE 4. Percent relative cumulative frequency versus azimuth velocity.

160°/sec in elevation, and at about 200°/sec in azimuth. At the other extreme, the data seem to show less activity at slow elevation rates than in azimuth; there are lower relative frequencies at the lower elevation rates.

The sampled head-position line-of-sight data are presented graphically for all subjects' trials in Figures 7 through 12. The data samples are shown by dots. The spread of the dots is indicative of the subject's head movement pattern. Subjects #1 and #3 have dot patterns that are fairly concentrated (Figures 7 and 9). Subjects #5 and #6 have dot patterns that are more dispersed (Figures 11 and 12), and subject #4 has dots spread generously over all the window areas (Figure 10). Subject #2's data were not useable because of a system malfunction (Figure 8).

No statistical analysis was done on the raw line-of-sight data, but the graphical presentations of these sampled data do provide a qualitative picture of the data collected.

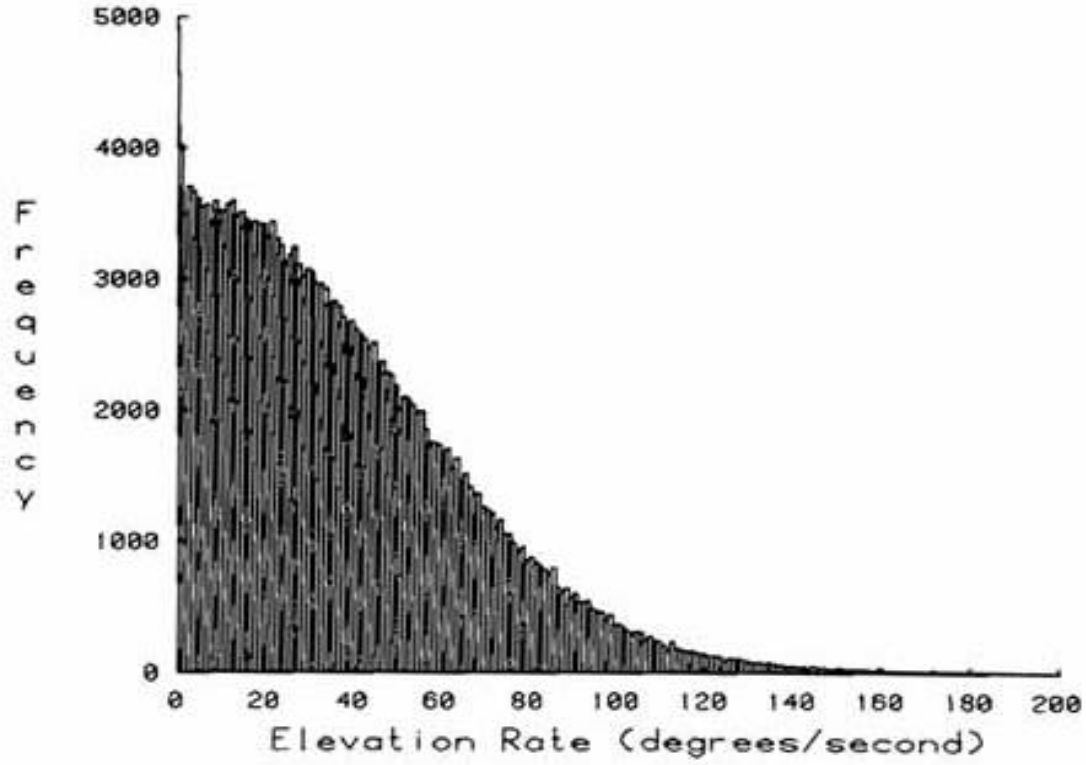

FIGURE 5. Frequency histogram for elevation velocity.

DISCUSSION

The head-movement data coi!ected during this experiment were tQ represent extreme movements that might be encountered during a very denonding flight mission. Before designing a mission and scenario that would meet the above goals, we had to determine the factors that influenced pilots' head movements in helicopters.

We began by observing pilots' head movements as they flew various missions in two different kinds of helicopters. There seemed tO be two factors that significantly influenced head movements. The first factor was aircraft configuration. Pilots had a different head-movement pattern when flying a tandem seat (single front and back seats) aircraft rather than a side-by-side seat aircraft. Window sizes and locations also were important configuration aspects that influenced head movements. Tandem seat aircrafts offer their crewmembers large viewing area[s,] and side-by-side seat aircrafts offer their crewmembers a "natural" vigilance responsibility area, a right side and a left side. Cockpit control and display configurations also influenced head movements.

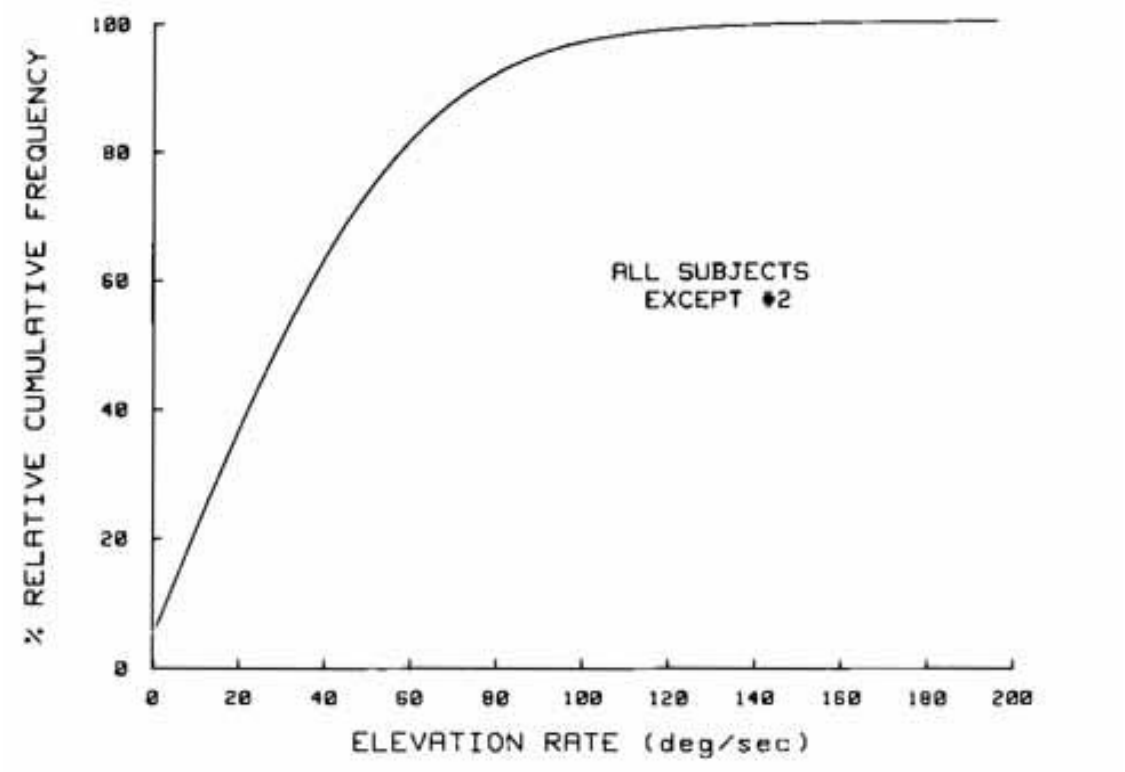

FIGURE 6. Percent relative cumulative frequency versus elevation velocity.

Table 1

Azimuth position frequency summary statistics
(azimuth expressed as degrees)

Subject	Trial	Mean	Median	S.D.	Skewness	Kurtosis
		θ		^	$\$_1$	$\$_2$
1	1	4.49	2.91	17.68	+0.105	+2.606
1	2	5.60	3.56	21.33	-0.247	+1.816
2	1	14.15	23.80	60.79	-0.343	-1.398
2	2	12.94	13.85	32.29	-0.540	+1.287
3	1	5.36	6.02	16.57	-0.742	+3.089
3	2	6.38	6.19	18.89	-0.219	+2.241
4	1	3.86	5.63	32.22	-0.448	+0.357
4	2	3.40	4.12	35.34	-0.292	-0.078
5	1	2.30	2.92	24.01	-0.512	+2.975
5	2	1.46	3.58	26.04	-0.919	+1.209
6	1	2.73	3.05	25.29	-0.650	+1.934
6	2	8.05	6.02	24.11	-0.440	+1.886
1	1¸2	5.05	3.23	19.62	-0.107	2.212
2	1¸2	13.56	15.67	48.85	-0.391	-0.663
3	1¸2	5.98	6.11	18.03	-0.368	2.568
4	1¸2	3.63	3.63	33.85	-0.361	0.121
5	1¸2	1.90	3.23	25.00	-0.736	2.044
6	1¸2	5.17	4.20	24.90	-0.567	1.941
Five subjects (#2 Not included)	1, 2	4.35	4.43	24.77	-0.523	1.933

Note 1: Subject #2 first trial had a malfunction in the mechanism.. The subject #2 second trial statistics suggested the possibility of further malfunctioning of the mechanism which may have been undetected at the time.
Note 2: Sample size for each trial was typically 20,000.

Table 2

Elevation position frequency summary statistics
(elevation expressed as degrees)

Subject	Trial	Mean	Median	S.D.	Skewness	Kurtosis
		0		$\hat{s}$	$\$_1$	$\$_2$
1	1	-4.16	-3.54	3.58	+0.172	8.715
1	2	-3.30	-2.70	4.05	+0.488	9.033
2	1	-0.09	+0.26	2.37	+1.634	36.121
2	2	+0.96	+1.77	4.22	-3.394	26.020
3	1	-3.09	-2.86	4.31	+0.575	6.6067
3	2	-2.99	-1.79	7.22	-2.894	17.442
4	1	-3.32	-1.84	8.98	-1.883	11.419
4	2	-9.35	-4.92	14.22	-1.233	1.020
5	1	-1.07	-0.11	8.04	-3.443	27.131
5	2	+1.31	+1.14	6.02	+1.311	3.666
6	1	+2.34	+3.56	7.95	-3.596	22.784
6	2	+4.06	+5.24	5.13	-2.524	17.037
1	1¸2	-3.73	-3.14	3.85	+0.397	8.964
2	1¸2	+0.44	+0.87	3.45	-2.566	31.548
3	1¸2	-3.03	-2.27	6.26	-2.642	19.953
4	1¸2	-6.39	-3.24	12.31	-1.618	3.547
5	1¸2	-2.32	+0.47	7.25	-2.319	24.309
6	1¸2	+3.13	+4.41	6.86	-3.666	26.323
Five subjects 1,2 (#2 is not included)		-2.09	-1.08	8.46	-2.249	11.787

Note 1: Subject #2 first trial had a malfunction in the mechanism. The subject #2 second trial statistics suggested the possibility of further malfunctioning of the mechanism which may have been undetected at the time.

Note 2. Sample size for each trial was typically 20,000.

Table 3

Azimuth angular velocity frequency summary statistics
for each subject and for each trial

Subject	Trial	Mean	Median	S.D.	Skewness	Kurtosis
		θ		$\hat{s}$	$\$_1$	$\$_2$
1	1	34.20	28.01	28.74	1.462	3.081
1	2	32.79	25.06	30.22	1.750	4.129
2	1	91.58	88.15	58.30	0.143	-1.186
2	2	30.21	20.38	33.00	2.244	5.929
3	1	32.00	25.71	28.16	1.671	4.079
3	2	34.39	28.19	29.02	1.454	3.038
4	1	38.03	27.80	36.55	1.732	3.342
4	2	36.89	25.93	37.04	1.736	3.200
5	1	41.20	34.25	33.62	1.355	2.333
5	2	39.92	32.93	33.28	1.419	2.575
6	1	38.55	31.46	32.69	1.458	2.717
6	2	32.13	23.89	31.22	1.906	4.673
1	1¸2	33.50	26.53	29.50	1.614	3.646
2	1¸2	43.64	25.97	47.31	1.549	1.594
3	1¸2	33.54	27.16	28.71	1.534	3.404
4	1¸2	37.44	26.85	36.81	1.733	3.264
5	1¸2	40.58	33.49	33.46	1.385	2.445
6	1¸2	35.60	27.69	32.18	1.639	3.428
Five subjects 1, 2 (#2 not included)		35.97	28.16	32.23	1.630	3.450

Note 1: Subject #2 first trial had a malfunction in the mechanism. The subject #2 second trial statistics suggested the possibility of further malfunctioning of the mechanism which may have been undetected at the time.
Note 2. Sample size for each trial was typically 20,000.

Table 4

Elevation angular velocity frequency summary statistics
for each subject and for each trial

Subject	Trial	Mean	Median	S.D.	Skewness	Kurtosis
		0		$\hat{s}$	$1	$2
1	1	37.30	32.46	28.05	0.956	0.883
1	2	35.19	29.50	28.11	1.270	2.198
2	1	34.45	29.01	27.47	1.242	2.080
2	2	29.14	24.70	23.24	1.273	2.478
3	1	33.17	28.35	25.87	1.071	1.371
3	2	39.58	34.87	29.18	0.926	0.856
4	1	35.55	30.10	28.32	1.319	2.601
4	2	35.99	29.34	30.70	1.529	3.125
5	1	46.07	40.35	34.41	1.090	1.405
5	2	41.10	37.02	29.27	0.848	0.697
6	1	42.23	37.83	30.58	0.996	1.299
6	2	31.20	26.41	25.31	1.419	3.354
1	1¸2	36.23	30.91	28.10	1.113	1.521
2	1¸2	31.83	26.77	25.61	1.297	2.425
3	1¸2	37.08	32.10	28.11	0.994	1.067
4	1¸2	35.78	29.71	29.57	1.446	2.959
5	1¸2	43.69	38.73	32.15	1.039	1.372
6	1¸2	37.16	32.08	28.81	1.186	1.980
Five subjects 1¸2 (#2 not included)		37.93	32.50	29.46	1.165	1.812

Note 1: Subject #2 first trial had a malfunction in the mechanism. The subject #2 second trial statistics suggested the possibility of further malfunctioning of the mechanism which may have been undetected at the time.

Note 2. Sample size for each trial was typically 20,000.

The aircraft suitably modified to conduct this study was a JUH-1M, a side-by-side seat aircraft, and the primary "beneficiary" of this study is the Apache, a tandem-seat aircraft. This inconsistency was addressed by stipulating the subject pilots' task. They were to fly the mission with minimal assistance from the safety pilot. Preliminary flights with test pilots confirmed the effectiveness of this stipulation. The test pilots could not rely on the safety pilot to monitor the aircraft's right side and were forced to scan it themselves.

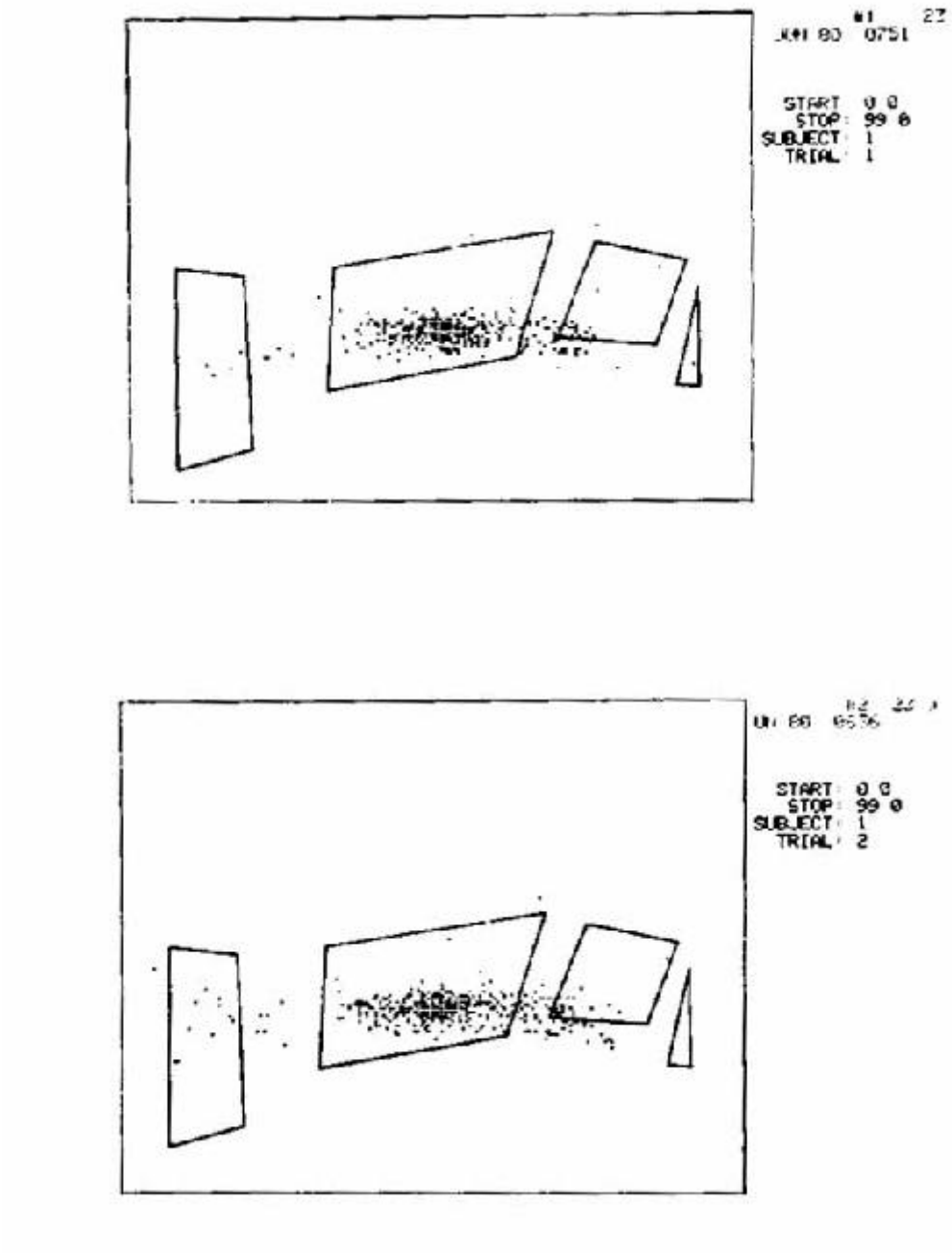

FIGURE 7. Line-of-sight data for subject #1. Data for trial A (top) and trial B (bottom) are provided.

The second factor that seemed to significantly influence head movements was the environment. Pilots had different head movement patterns when "ciearing themselves" for takeoff or landing, when flying in friendly rather than "enemy" territory, and when flying in a familiar, rather than an unfamiliar, area.

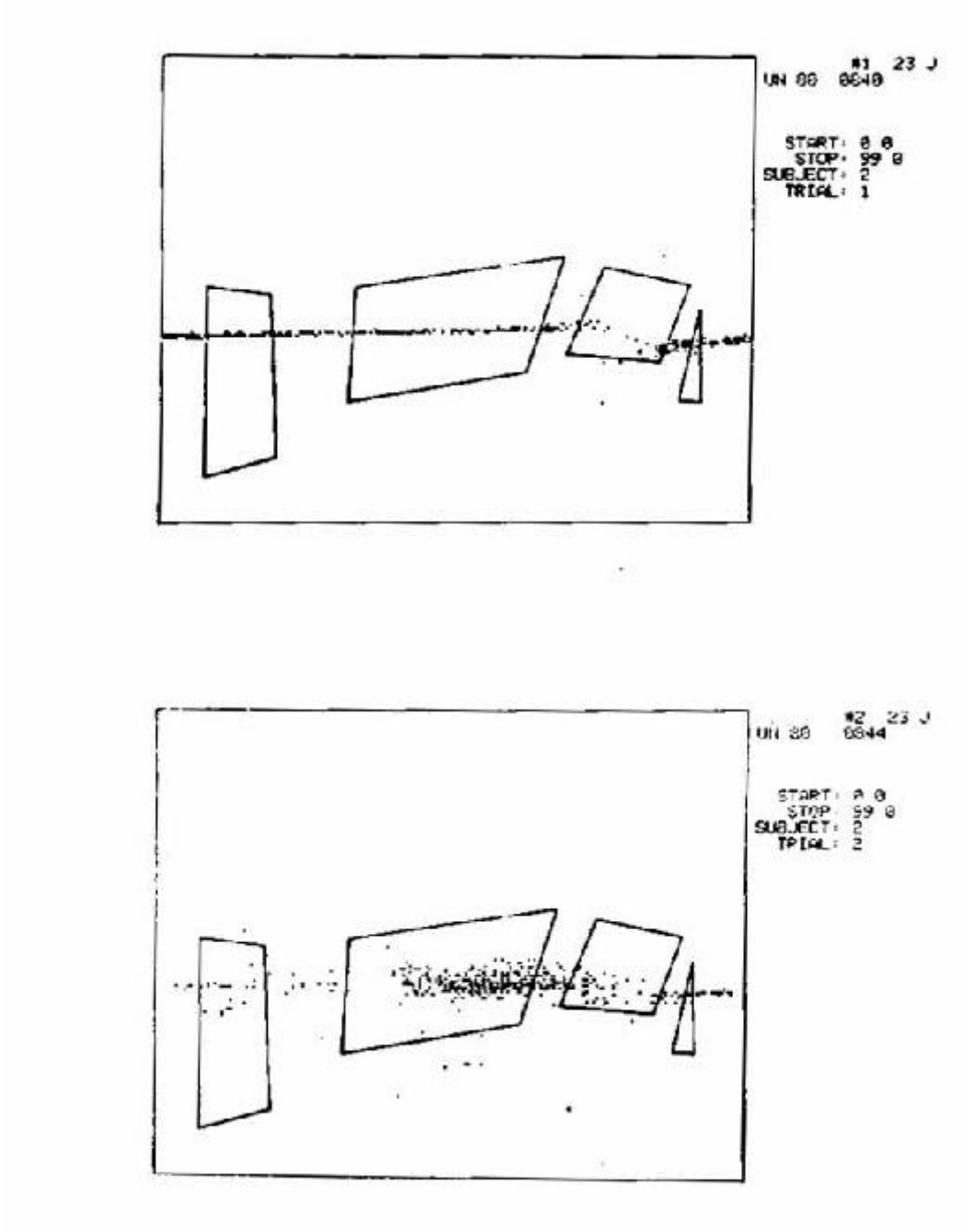

FIGURE 8. Line-of-sight data for subject #2. Data for trial A (top) and trial B (bottom) are provided.

A contour flight which included a threat aircraft provided a plausible and demanding mission/scenario for the experiment.

Although the primary purpose of the experiment was to gather head-rate data, its byproduct, the head-position data, also provided some useful information (Figures I and 2). Approximately 50 percent of the position data was within -7° to 12° azimuth and -5° to 1° elevation, a very small area considering

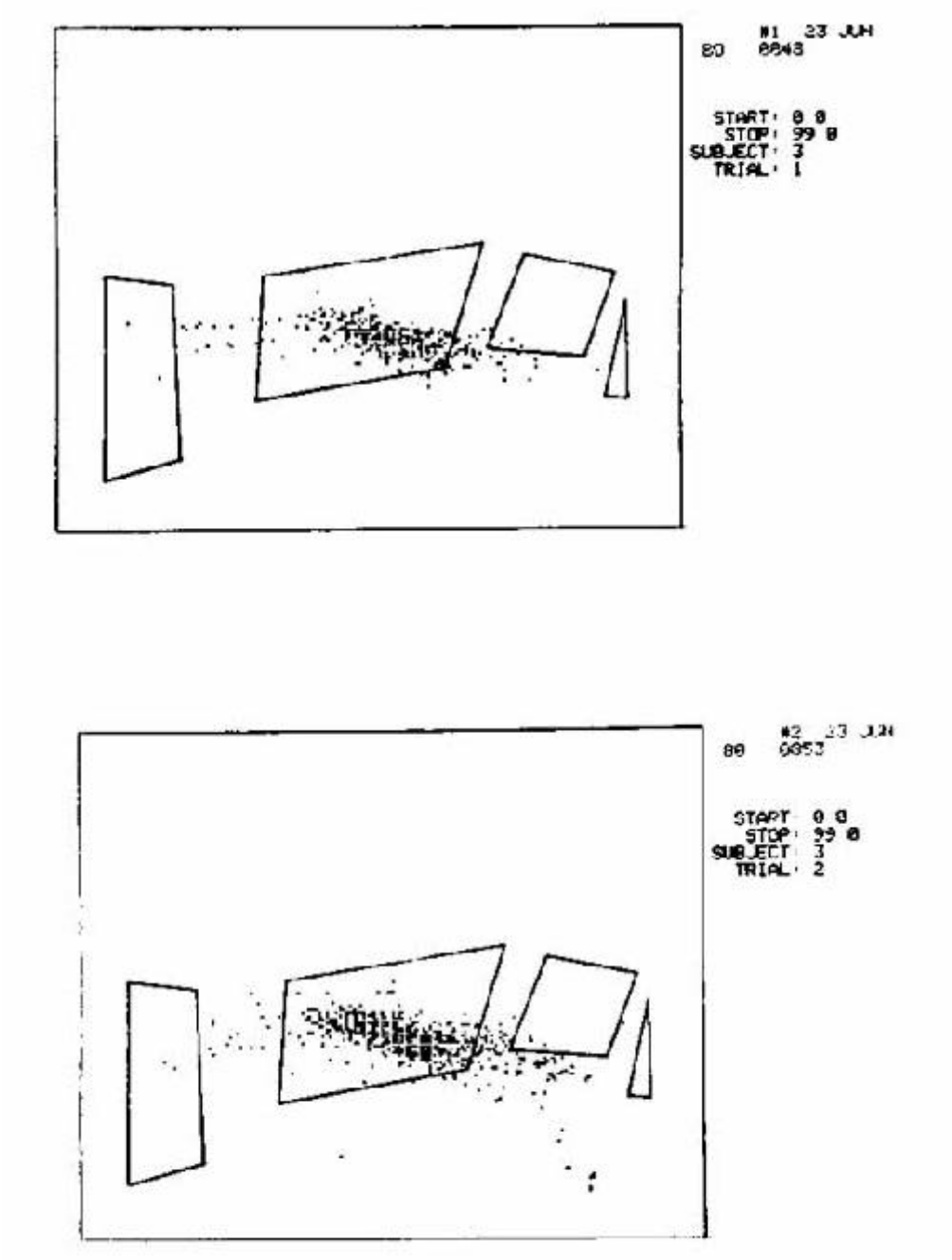

FIGURE 9. Line-of-sight data for subject #3. Data for trial A (top) and trial B (bottom) are provided.

the pilot's task. However, it must be remembered that the head position must pass through center for all side-to-side and most up and down head movements.

The maximum azimuth excursions of the pilots' heads were within +/-80°, indicating that the pilots used only head-neck turns, since their torsos probably were constrained by the seat and safety harness. The maximum negative elevation excursions, to -75°, were outside the -10° head-only position limits, indicating that the neck participated in the negative angle movement

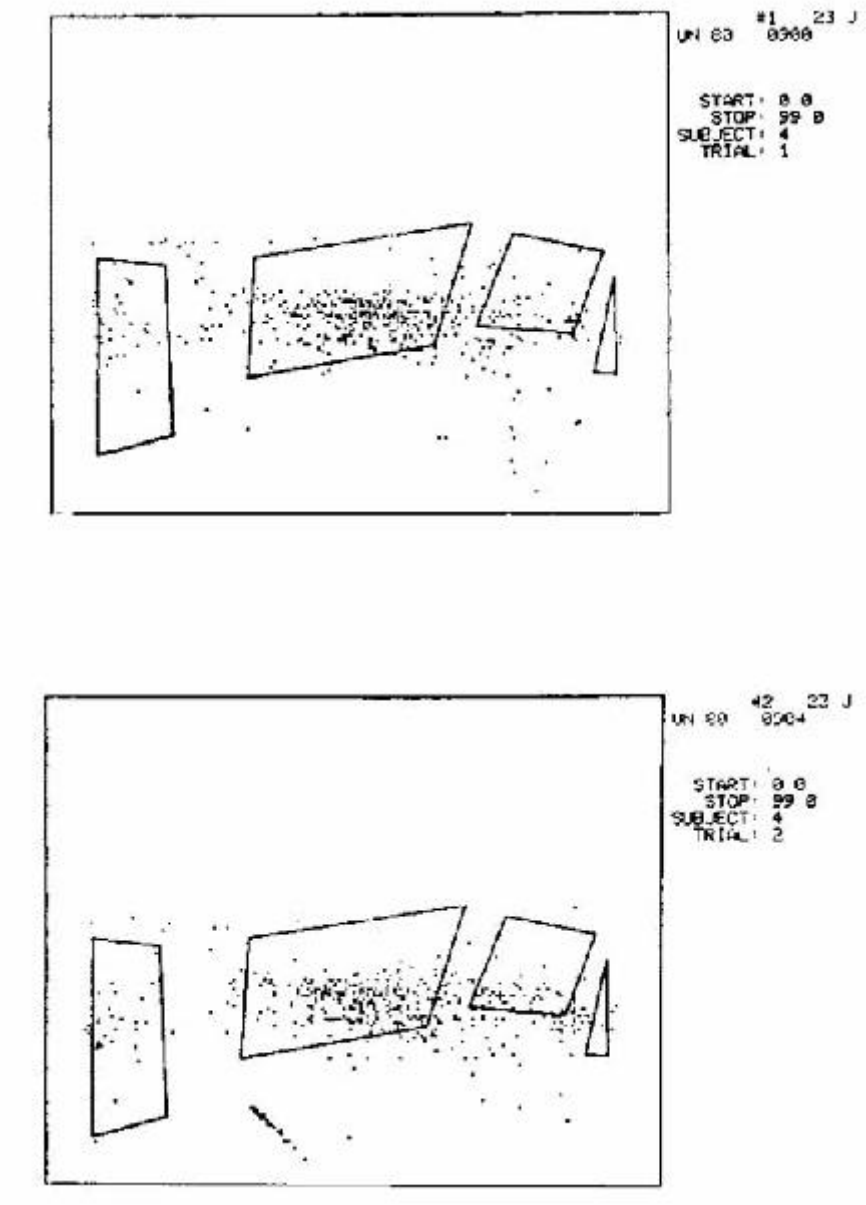

FIGURE 10. Line-of-sight data for subject #4. Data for trial A (top) and trial B (bottom) are provided.

(Caillient, 1981). The large positive elevations, to 30°, probably resulted from the subjects' search for the hostile chase aircraft.

The angular velocity data suggest that even with greatly different head-movement patterns, the head velocity ranges are relatively constant. Head positioning time seems to be an important underlying consideration. The head's control system increases the velocity of the turn movement so that the head is positioned at the desired location within a specific time constraint. If the

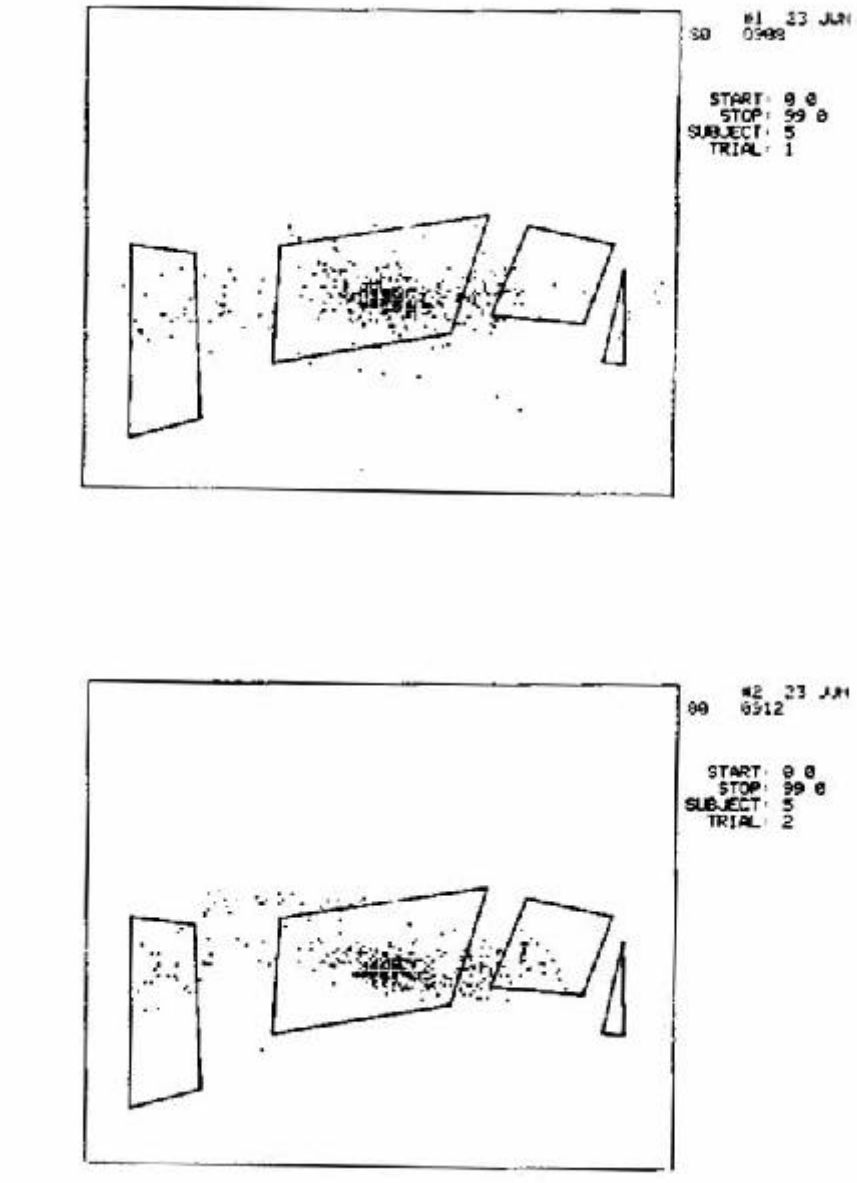

FIGURE 11. Line-of-sight data for subject #5. Data for trial A (top) and trial B (bottom) are provided.

future location is far from its present location, the velocity of the movement will be greater than if the future location is closer (Zangemeister and Stark, 1981).

The behavior of the azimuth and elevation mechanisms seems relatively symmetric (Figures 4 and 6). The cumulative relative frequency data for the azimuth rates differ from the elevation rate data by less than one percentage point for all calculated rates.

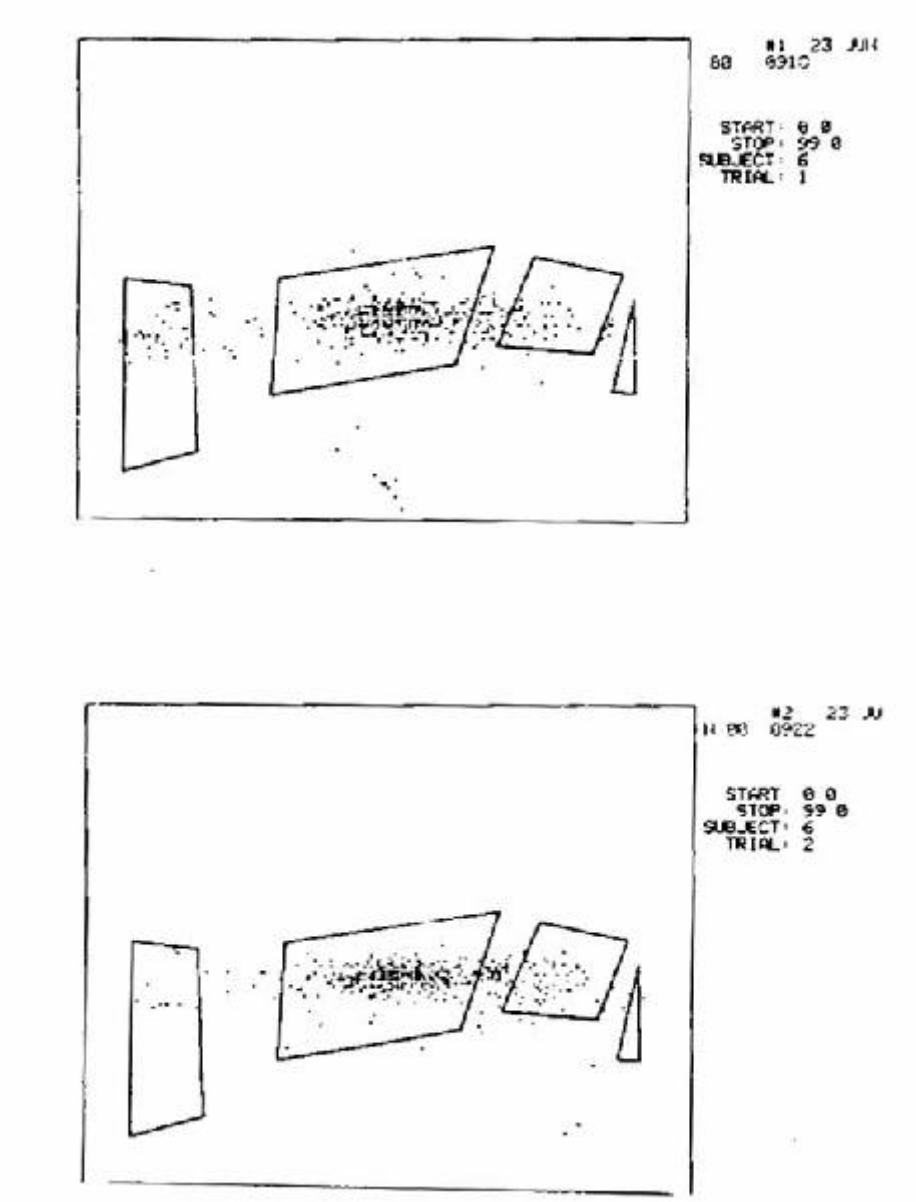

FIGURE 12. Line-of-sight data for subject #6. Data for trial A (top) and trial B (bottom) are provided.

The velocities observed were, at most, 60 percent of the head's maximum capacity (352//sec). Related to the design specification of the Apache VCS, the range between O^{O}/sec and 120//sec would account for about 97 percent of the azimuth rates and 98 percent of the elevation rates measured during the trials.

In the graphic head position illustrations (Figures 7 through 12), some dots represent actual line-of-sight eye fixations, and other dots mark transition points as the pilot was turning his head from one fixation area to another. For the purposes of this study, the difference is unimportant, but it does help to explain some of the dots locations.

Some dots are projected on the JUH-1M's primary windows, and others are projected on undefined areas of the figures. These undefined areas include controls, displays, and structures. The dots on the aircraft structures (e.g., spaces between windows) are transitional head positions. When viewing the graphical presentation as it is presented on a computer display "live," one can see the sequential movements of the pilot's head.

CONCLUSIONS

The concentration of the azimuth and elevation data points indicated that the pilots looked primarily forward, even though the scenario required a broad range of head movements; however, this concentration is influenced by the transitional data points. The pilots exhibited search patterns, and the resultant position/velocity variation between subjects was small and of no practical significance.

The head-position data suggested pure head-neck movements without torso participation. The seat and safety harness probably restricted the torso movements too much to make it a practical participant.

The angular velocity data support the 120O/sec head movement rate used in the Apache's specifications. Approximately 97 percent of the measured azimuth and 98 percent of the elevation angular rates were equal to or less than 120//sec. The experimental velocity data also support the symmetry of the azimuth and elevation head movement components.

REFERENCES

Allen, John H. and Webb, Richard C. 1983. *Helmet mounted display feasibility model.* Orlando, FL: Naval Training Equipment Center. NAVTRAEQUIPCEN IH-338.

Caillient, Rene. 1981. *Neck and arm pain.* Philadelphia, PA: F.A. Davis Company.

Johnson, John C., Priser, David B., and Verona, Robert W. 1981. *Vibration in a helmet mounted sight using mechanical linkage.* Fort Rucker, AL: US ArITLV Aeromedical Research Laboratory. USAARL Report No. 81-3.

Phillips, Chandler A. and Petrofsky, Jerrold S. 1983. Quantitative electro-myography: response of the neck muscles to conventional helmet loading. *Aviation, Space and Environmental Medicine.* May 1983, pp 452-57.

Verona, Robert W., Johnson, J. C. and Jones, Heber. 1979. *Head aiming/tracking accuracy in a helicopter environment.* Fort Rucker, AL: US Army Aeromedical Research Laboratory. USAARL Report No. 79-9.

Zangemeister, Wolfgang H. and Stark, Lawrence. 1981. Active Head Rotations and Eye-Head Coordination. *Annals of New York Academy of Sciences.* 374:541-59.

APPENDIX A

Modeling Aviator Head Movement

INTRODUCTION

A mathematical modeling endeavor is an attempt to "explain" a body of data and facts in mathematical terms. The *mathematical terms* are used in the sense of translating real world problems into a mathematical one by making a number of simplifying assumptions, and by making use of the shorthand notation and a set of operators, e.g., addition and multiplication, from mathematics. One of the goals of this note is to construct a stochastic model, *i.e.*, a probability model, of the head movement of helicopter aviators while they are engaged during flight in searching for another helicopter also in flight.

The data presented in the text gives the empirical or observed frequency distribution of both the position of the head and the velocity of the head motion. The text Figures 1 and 2 give the head azimuth and elevation position, respectively. The text Figures 3 and 5 give the head azimuth velocity and the head elevation velocity, respectively. These figures represent the frequency distributions "summed" for five of the subjects on which the measurements were made. These data, plus the individual histograms for the five aviators, were the basis for the particular models chosen. The modeling process was guided to a very large extent by the graphical representation of the data. To a lesser extent, the summary statistics given in the text Tables 1, 2, 3, and 4 provided a guide to the modeling activity.

What was desired from the modeling work were probability distribution functions (p.d.f.) given the data exhibited in the frequency diagrams and exhibited in the summary statistics. These p.d.f., which will be called distribution throughout the sequel, were required to mimic or echo the physical/biomechanical aspects of the system, *i.e.*, the human head in motion while searching. In other words, the distributions are required to "make sense." A word of caution is needed at this point. A dictum formulated by Dr. G. E. P. Box states: "All models are wrong, some are useful." The essence of the problem is, then, to construct or derive some distributions or density functions from the empirical distributions observed. These mathematical probability distributions are stochastic models of the phenomenon.

An alternative approach to the modeling might have been entertained. The alternative approach is the modeling of the head's motion using deterministic equations such as differential equations or partial differential equations. Such an approach and subsequent model is illustrated by Marshall (1984) in which he gives the dynamical equations for the stride swing in human walking.

What will be presented in this note are: briefly, the mathematical tools used, the distributions for head position and velocity, a discussion of these distributions, and a summary.

METHODS

The methods used fall into two categories. These are not necessarily mutually exclusive, at least in the manner that they were used. The first method is mathematical statistics. The second method consists essentially of graphical analysis, especially the fitting of mathematical distributions to the observed distributions. The graphical analysis actually goes beyond the mere curve fitting procedure in that the interaction of graph, eyes, and brain were used to assess, assimilate, "digest," and finally interpret the significance of graphical analysis process/results.

The elements of the mathematical statistical methods can be found in such texts as Feller (1971), Freund (1971), Kendall and Stuart (1963), and Wilks (1962). Material in the texts by Parzen (1960) and Tsokos (1972) played a large role in the development of the stochastic models. The primary statistical element used was, obviously, the definition of a probability distribution function and concept of a random variable (r.v.). The concept of an r.v. will not be dwelt upon here, but the interested reader can pursue that concept in the several texts cited above. Moreover, a continuous r.v. will be considered throughout the sequel as opposed to discrete r.v.s, e.q., Poisson variable.

Thus, for a continuous r.v. in one dimension, the following short definition of a p.d.f. is used:

$$\Pr(\alpha \le X \le \beta) = \int_{\alpha}^{\beta} f(x)\,dx \qquad (1)$$

where Pr is an abbreviation for *probability*, X is a r.v., α and β are real numbers such that $\alpha < \beta$, $f(x) \ge 0$, for all $x \in R_x$, the range space, and $\int_{R_x} f(x)dx = 1$.

Using equation (1), given a suitable f(x), and some theorems from mathematical statistics, statistics such as the mean, median, or variance of a distribution can be obtained. Moreover, statistics such as the β_1, a measure of skewness, i.e., departure from symmetry, and β_2, a measure of kurtosis, i.e.,the "flatness" or "peakedness" of a distribution, can be derived. However, the function f(x) is the major element in the development of the model that is important. For the data in the text proper, finding a function, f(x), that satisfies the definition and provides a reasonable model or “explanation” of the phenomenon is the real objective of the exercise. Furthermore, the function chosen should be as parsimonious as possible, *i.e.*, as few parameters possible are used consistent with the actual circumstances of the physical/ biological aspects of what is observed or measured.

For example, given the data for the frequencies shown in the text Figure l, a polynomial function could be found that would "fit" the observations perfectly and, with a dint of effort, the resultant n-1 degree polynomial could be modified so as to meet the definition in equation (1) above. However, the degree of the polynomial for the azimuth position of the head would possibly be greater than three. Moreover, the same degree polynomial might not fit the elevation position of

the head very well. In the main, a reasonable person would prefer a function with very few parameters over that with several adjustable constants.

Not too much detail about the graphical analysis will be presented in this section since it can be better explained in the results section when actually citing the several figures and the graphs contained in them. The graphical analysis was done using programs written in BASIC or modifications of such programs for a microcomputer. This computer permits the display of graphs on a CRT and its peripheral equipment permits hardcopies to be made of the graphs displayed or pen-and-ink graphs to be made on a XY-plotter. The latter system was used to make the several graphs displayed in the accompanying figures to this appendix.

One final item about the graphical analysis is worth mentioning. It was done iteratively until a suitable, but subjective, point of convergence was reached. The particular point of convergence was chose *ad libitum* or *arbitrium.*

Although the text gives data for five subjects, the results presented here will focus almost exclusively on subject three's head motion measurements. The data for subject three is believed to be "typical" of the data for subjects 1, 3, 5 and 6. Subject four's data are atypical and that data will be discussed in the sequel. Since the measuring apparatus malfunctioned during the run, subject two's data was not considered. Table A-1 gives the summary statistics for subject three's data. The descriptive statistics were extracted from the text Tables l, 2, 3, and 4.

RESULTS

By way of an introduction to the results of the modeling process, consideration is given to the global aspects of human head motion and the manner in which the measurements were made in this study. If the human head is thought of as a globe or sphere which is permitted to move on a flexible shaft (the neck) within certain constraints on the degree that the glove can move either laterally or sagittally, then the head can be thought of as having both rotational motion and translational motion or combinations of these.

TABLE A-1

SUMMARY STATISTICS FOR SUBJECT 3: AZIMUTH AND ELEVATION POSITION AND VELOCITY

Trial	Sample Size	Mean	Standard Deviation	Median	Skewness	Kurtosis	Interquartile Range
	N	$\bar{0}$	$\hat{s}$	$\tilde{x}$	$\hat{b}_1$	$\hat{b}_2$	$Q_{75} - Q_{25}$
			Azimuth Position (degrees)				
1	21104	5.36	16.57	6.02	-0.742	3.089	13.454
2	33256	6.38	18.89	6.19	-0.219	2.241	15.709
			Elevation Position (degrees)				
1	21104	-3.09	4.31	-2.86	0.575	6.067	5.038
2	33256	-2.99	7.22	-1.79	-2.894	17.442	5.995
			Azimuth Velocity (degrees/second)				
1	21214	32.00	28.16	25.71	1.671	4.079	33.808
2	32934	34.39	29.02	28.19	1.454	3.038	37.062
			Elevation Velocity (degrees/second)				
1	21071	33.17	25.87	28.35	1.071	1.371	35.536
2	32965	39.58	29.18	34.87	0.926	0.856	41.016

However, the manner in which the measurements were taken are such that the head, as a fictional globe, moved *as if* it were mounted on gimbals such that the head moved only left or right in the equatorial plane of the globe, or up and down in the polar plane of the globe. What has been described is shown in the following diagram:

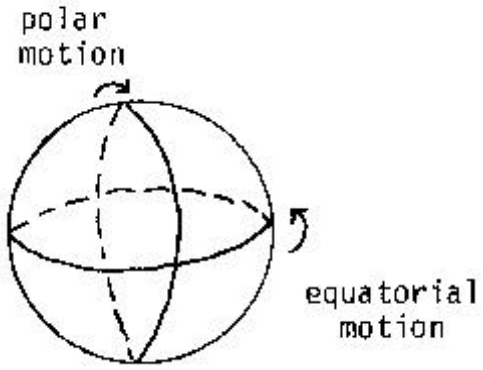

The head motion can be viewed *as if* a fixed light ray emanates from the center point of a sphere which rotates sideways, and up or down, and the end point of the ray makes a track upon a spherical "universe" or" canopy." The movement of this point of light on the spherical universe is recorded with respect to an x,y coordinate system with the origin at the center of the sphere. The velocity of the point of light--the end of the light ray--also is recorded as it moves to and fro on the spherical universe. Thus, the head motion actually recorded via the measuring system is different from that of the true motion of the head which includes the ability of the head to "tilt" or "cant." This somewhat artificial head motion--the motion of the fictitious globe or sphere--must be kept in mind when reading the results of the models developed.

The results will be presented in two subsections. The first will give a model for the head position, while the second will give the results for models of the head velocity.

HEAD POSITION MODEL

Text Figures 1 and 2 display the histograms from the azimuth (side-to-side) position of the head and the elevation (up and down) position of the head, respectively. These histograms have nearly identical shapes and configurations. This suggests that the same distribution can serve as a model for either of the two positions.

The distribution model considered for the head position is the Cauchy distribution. The Cauchy distribution may be expressed in the following way, using the notation of Wilks (1962)'

$$f(x;q_1,q_2) = \frac{1}{p} \cdot \frac{q_2}{\left[q_2^{\,2} + \left(x - q_1\right)^2\right]}, -\infty < x < \infty \qquad (2)$$

where 2_1 is a location parameter and 2_2 is a scale parameter. Hasting and Peacock (1975) give a formula for the Cauchy distribution, some of its attributes and a method for generating the distribution using the ratio of two normal distributions, i.e., N(O, 1). The Cauchy distribution can be developed as follows (Tsokos, 1972).

In the tableau below, assume that a randomly chosen straight line is drawn through the point $(2_1,2_2)$. It hits the x-axis at the point (x, 0), making an angle of R with the 2_2-axis. Assume that R varies from -(B/2) to +(B/2).

$$f(y) = \begin{cases} \dfrac{1}{p}, & -\dfrac{p}{2} \le y \le \dfrac{p}{2} \\ 0, & elsewhere. \end{cases} \tag{3}$$

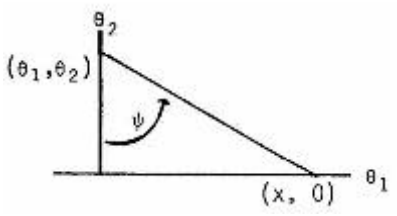

To find the density of the random variable X, where x - e1 = e2 tan 4, the following is done:

$$h(x) = f(y)\left|\frac{dy}{dx}\right|, \tag{4}$$

where

$$\frac{dy}{dx} = \frac{1}{q_2 \sec^2 y} = \frac{1}{\dfrac{q_2\left[q_2^2 + (x-q_1)^2\right]}{q_2^2}} = \frac{q_2}{q_2^2 + (x-q_1)^2} \tag{5}$$

Note that when R = -(B /2), x = - 4; and when R = +(B / 2), x = +4. Therefore,

$$h(x) = \frac{1}{p} \cdot \frac{q_2}{\left[q_2^2 + (x-q_1)^2\right]}. \tag{6}$$

The function h(x) is, of course, equal to the function given in equation (2). As is well known, the Cauchy distribution does not have finite moments, i.e., the, mean, variance, etc., of the Cauchy distribution do not exist. The estimation of G1 and e2 will be discussed in the sequel.

To illustrate one of the reasons why the Cauchy distribution was chosen instead of the Gauss, or Normal, distribution, consider this example. A BB gun or machine gun is mounted at the point $(0, \theta_2)$ on a bench so that it can freely swing 180^o. The gun fires its ammunition at a straight line marked on a board directly in front of the bench. If all angular positions of the gun are equally likely, i.e., has a uniform circular p.d.f., then the distribution of hits will follow a Cauchy distribution. The motion of the head, within the constraints described in the methods section, can be likened to the gun swiveling to and fro with the "hits" being a record of where the head is facing as it searches outward from the cabin of a helicopter. Mention is made of another physical analogy for the Cauchy distribution which is given in a footnote on page 51 of Feller (1971). The analogy is that if a unit light source is situated at the origin, then h(x) represents the distribution of the light along the line y = t of the x,y-plane. The convolution of $h(x)_t * h(x)_s = h(x)_{s+t}$ expresses *Huygens' principle,* according to which the intensity of light along y= s + t is the same as if the source were distributed along the line y= t following the Cauchy distribution $f(x; \theta_1, \theta_2.)$.

The data for subject three is a finite sample which is assumed to have been drawn from a Cauchy distribution. Because the Cauchy distribution does not have a mean or variance as does the Gauss distribution, hence, a problem exists of estimating values for the parameters θ_1 and θ_2. According to Wilks (1962), the parameter θ_1 is estimated by the sample median while the parameter θ_2 is estimated by the sample interquartile range, $Q_{75} - Q_{25}$. However, Johnson and Kotz (1970) show that θ_2 is estimated by one half the interquartile range and 91 is, as Wilks states, estimated by the median. These estimators were used, for the most part, in fitting the Cauchy distribution to the azimuth and elevation position histograms. However, the means instead of the median gave a slightly better estimate of θ_1; but this is not surprising since for a symmetrical distribution the median coincides with the mean value for a large sample size.

The estimates of the parameters are given in Table 2-A. The reader is invited to read the footnotes on Table 2-A, especially those concerning the elevation position, trials 1 and 2. The iterative graphical analysis suggested the estimates which were actually (end products) used in the graphical fitting process.

The results of fitting the Cauchy distribution are displayed in Figures A-1 and A-2 for the azimuth position, Trials 1 and 2, respectively. Figures A-3 and A-4 display the results of fitting the Cauchy distribution to the elevation position data, Trials 1 and 2, respectively. The goodness of fit or lack of fit will be addressed in the discussion section.

TABLE A-2

ESTIMATES * OF PARAMETERS FOR THE CAUCHY,
MAXWELL AND GAUSS' (NORMAL)
PROBABILITY DISTRIBUTION FUNCTIONS: SUBJECT 3 DATA

Cauchy Probability Distribution Function
(estimates)

Parameters: 1_1 (= 0) 1_2 [= ½ (interquartile range)]

Azimuth Position

Trial 1	5.362	6.727
Trial 2	6.377	7.844

Elevation Position

Trial 1	-2.856	2.758 [= ¼ (5.038 + 5.9951]**c**
Trial 2	-1.803	3.304 [= ¼ (5.995 + 7.223)]Š

Maxwell Probability Distribution Function (estimates for folded distribution)

Parameter	N'	1/" = F	M(z)**
Azimuth Velocity			
Trial 1	42428	41.821	1.64
Trial 2	65868	43.095	1.64
Elevation Velocity			
Trial 1	42142	38.408	1.96
Trial 2	65930	43.328	1.96

Gauss(Normal) Probability Distribution Function(estimates for folded distribution)

Parameter:	: = mode	F	M(z)**
Azimuth Velocity			
Trial 1	2.00	28.164	1.28
Trial 2	2.00	29.022	1.28
Elevation Velocity			
Trial I	2.00	25.866	1.64
Trial 2	2.00	29.179	1.64

* Estimates were obtained from the summary statistics given in Table A-1.

c A weighted estimate derived from the interquartile ranges of Trial 1 and Trial 2.

Š A weighted estimate derived from the interquartile range of Trial 1 and the standard deviation of Trial 2.

** The N (z) is the cumulative Normal Distribution Function (see text for explanation).

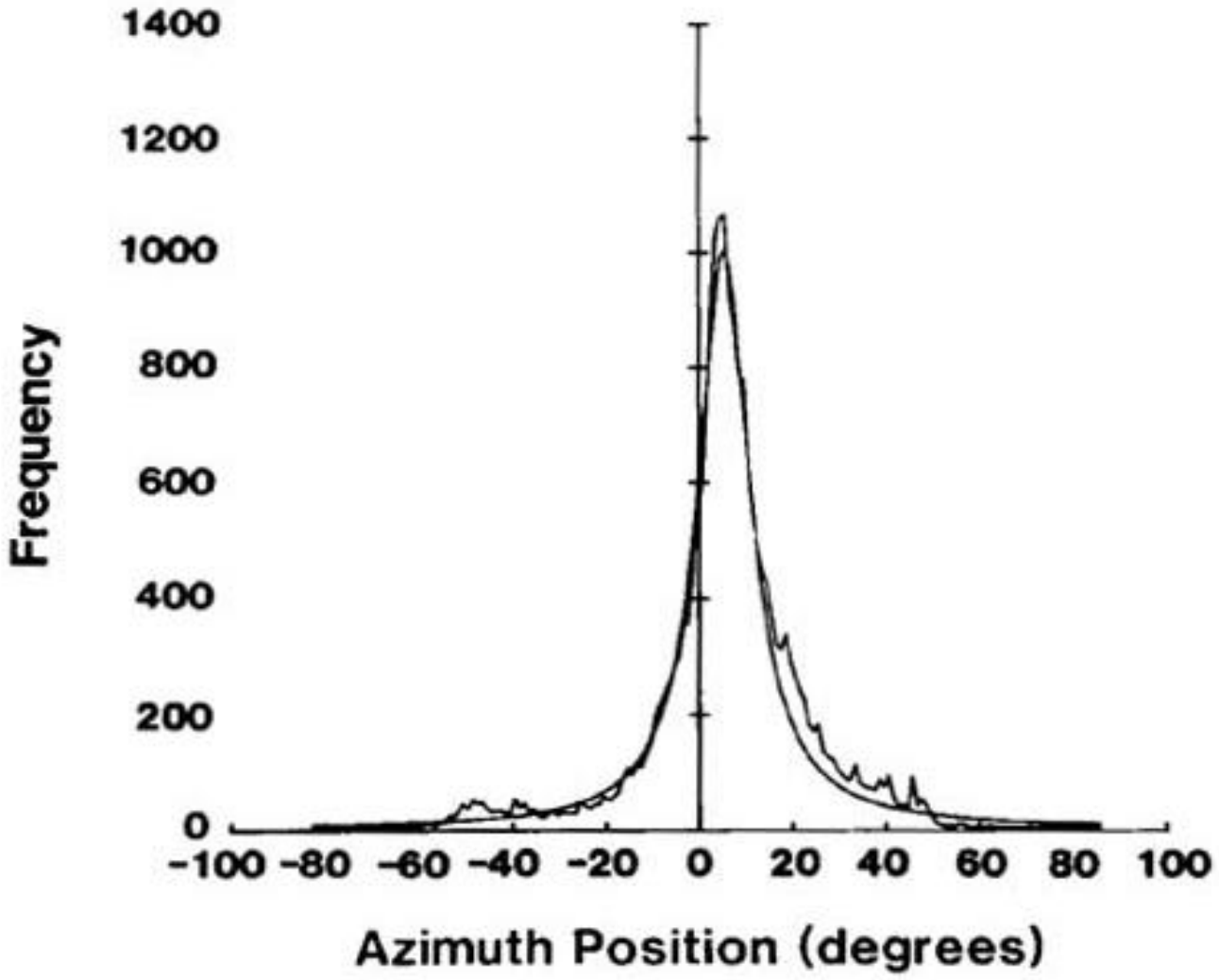

FIGURE A -1. Azimuth head position frequencies and the fitted (smooth curve) Cauchy distribution for Subject 3, Trial 1.

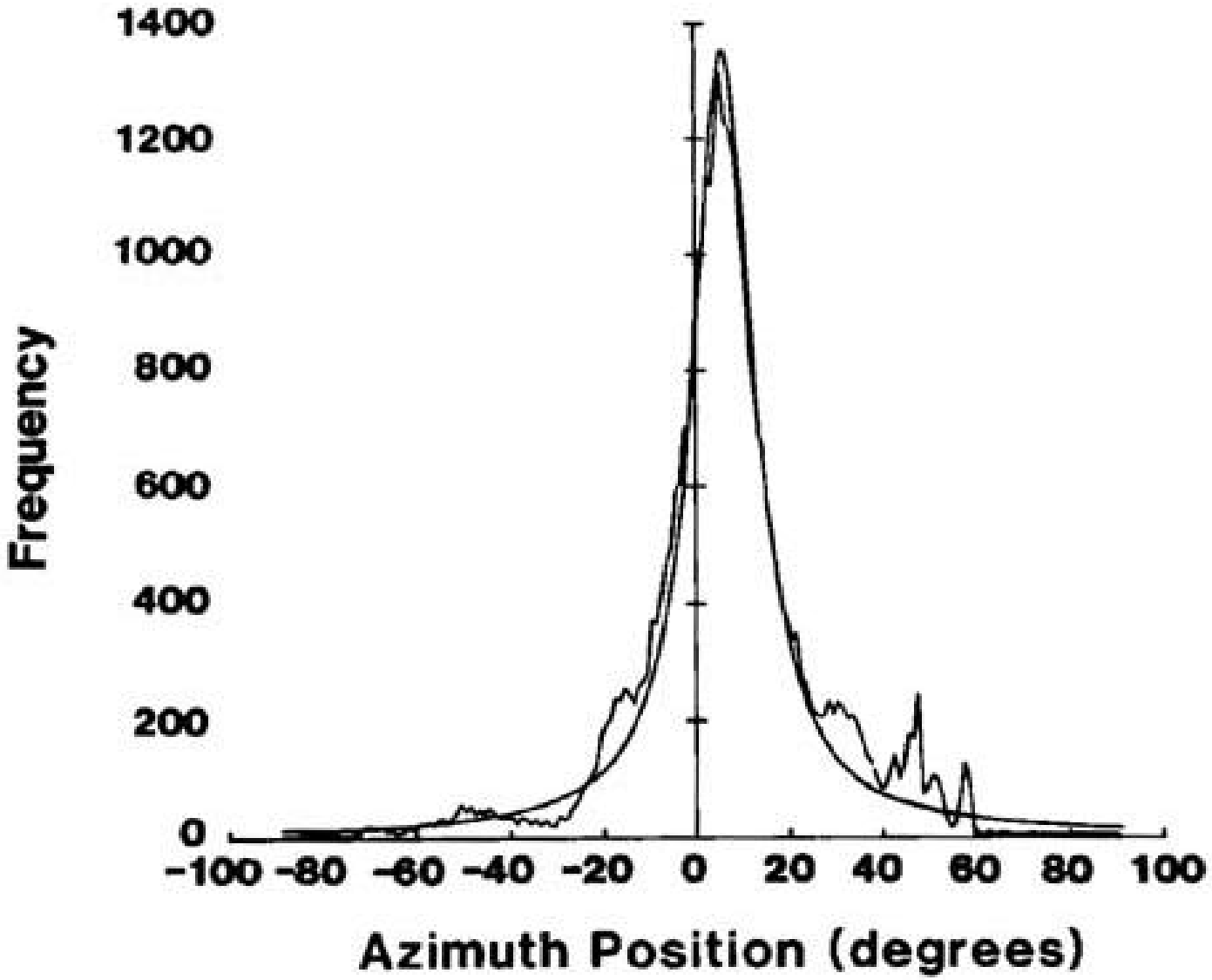

FIGURE A-2. Azimuth head position frequencies and the fitted (smooth curve) Cauchy distribution for Subject 3, Trial 2.

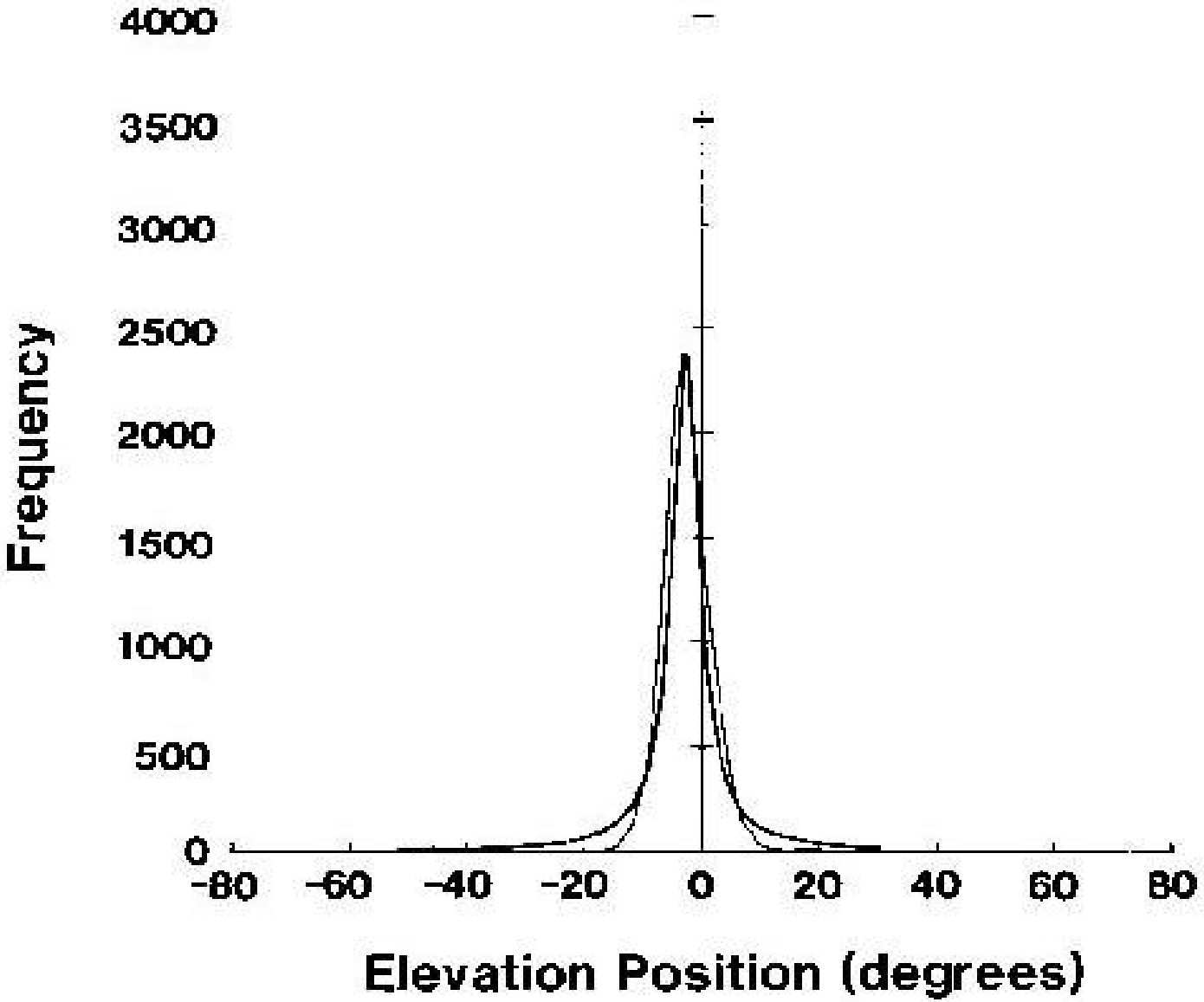

FIGURE A-3. Elevation head position frequencies and the fitted (smooth curve) Cauchy distribution for Subject 3, Trial 1.

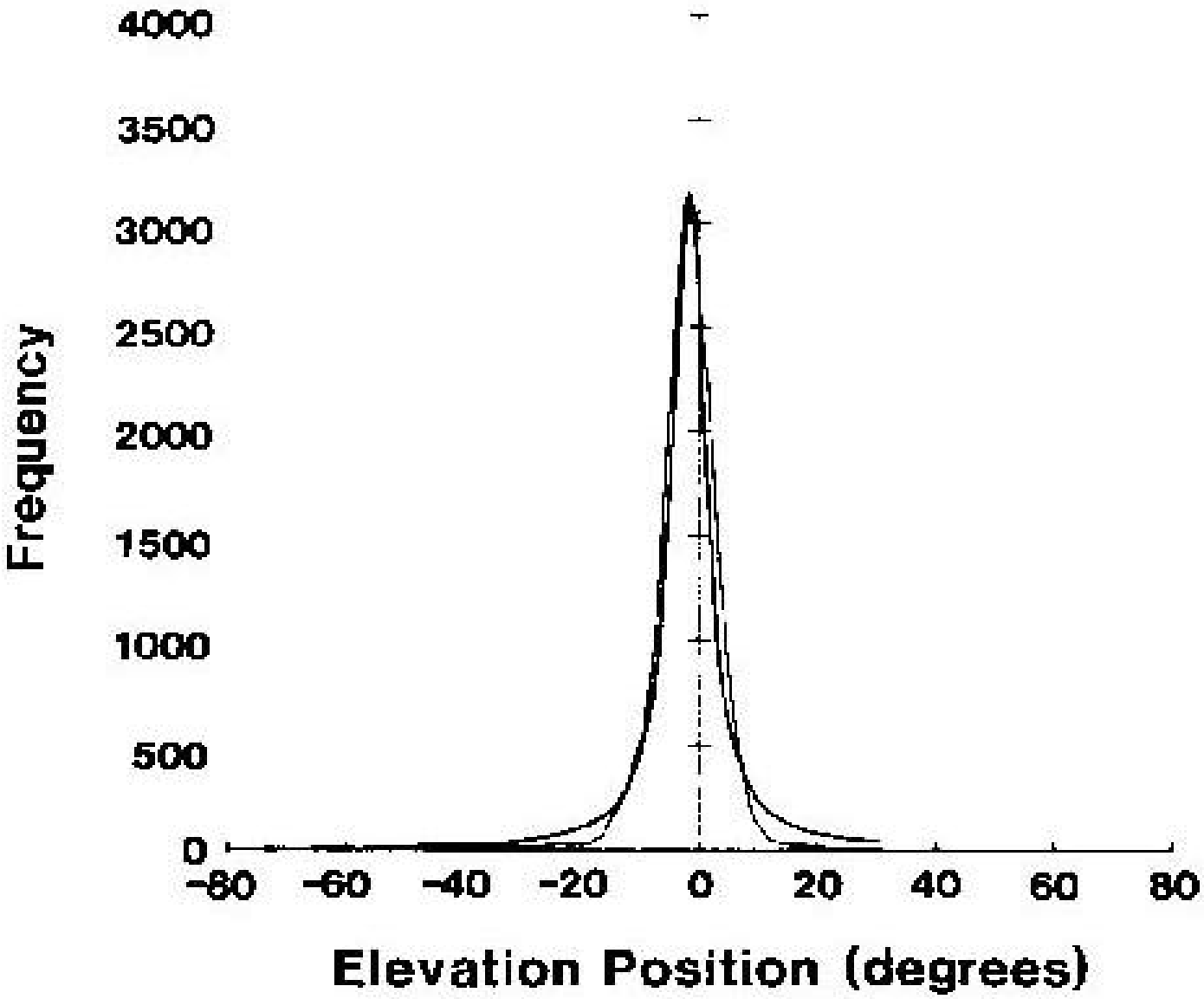

FIGURE A-4. Elevation head position frequencies and the fitted (smooth curve) Cauchy distribution for Subject 3, Trial 2.

HEAD VELOCITY MODELS

Text Figures 3 and 4 display the histograms for the azimuth head velocity and elevation head velocity, respectively. As in the case of the head position graphs, these histograms have nearly identical shapes and configurations. This suggests that the same distribution can serve as a model for either of the two velocities, i.e., azimuth (side-to-side) velocity or elevation (up and down) velocity.

The text figures also suggest, among other things, that what is presented is either the right-hand portion of a truncated distribution or a symmetrical distribution that has been folded in half, *i.e.*, the left-hand side folded on top of the right-hand side. A folded distribution is possibly the more likely of the two. Dr. A. B. Forsythe, in a personal communication, suggested that what actually is presented in the text figures is a folded distribution of velocities in which velocities of the head moving to the left are mixed in with the velocities of the head when moving to the right (the word up or the word down can be substituted for left and right, respectively, for the case of the elevation velocities).

Moreover, if the distribution is a folded one, then the shape of the right-hand portion suggests that of the shape of a bell-shaped curve which is, of course, one way of describing the Gauss distribution or so-called Normal distribution. In fact, Dr. G. E. P. Box suggested that possibility during a conference in April 1984 at the Mathematics Research Center, Madison, Wisconsin. However, when dealing with velocities for statistical analysis purposes in an analysis of variance, a recommendation often is made to transform velocity data so as to stabilize the variance. This would not be necessary if velocities were a sample (large) drawn from a Gauss distribution. This fact suggested that a different, but related distribution may be a more appropriate one.

The Maxwell probability distribution function for the velocities of gas molecules is a likely candidate for the distribution of head motion velocity albeit the human head hardly has the mass of a gas molecule. The Maxwell distribution, according to Sears and Zemansky (1963) can be written as a differential equation (D.E.):

$$\frac{dN}{dv} = \frac{4N}{\sqrt{p}}\left(\frac{m}{2KT}\right)^{3/2} v^2 \exp\left[-\left(mv^2 / 2KT\right)\right] \qquad (7)$$

where N is the number of gas molecules, v is the molecule velocity, m is the molecule mass, T is absolute temperature, K is the Boltzmann-Maxwell-constant, and B and exp (= e) have their usual mathematical definitions. The D. E. form of the Maxwell distribution is displayed to indicate that the distribution may be useful to model head motion velocity since the mass of the head could be substituted for m, the molecule mass. Also, the aviators flew in a particular heat regimen that could be expressed in terms of T, the absolute temperature.

Parzen (1960) and Tsokos (1972) both give a p.d.f, for the Maxwell distribution which differ only in appearance and notation. Parzen's function is:

$$f(x;a = \begin{cases} \frac{4}{\sqrt{p}} \frac{1}{a^3} x^2 \exp\left[-\left(x^2 / a^2\right)\right]; x \geq 0, a > 0 \\ 0, \text{ elsewhere} \end{cases} \quad (8)$$

where x = v, the velocity in equation (7); " is the parameter of the distribution which is to be estimated. A considerable amount of detail for this distribution is found in Appendix B. Certain additional aspects of the Haxwell distribution as a model for head motion velocity will be cited in the discussion section.

The distribution function given by equation (8) is not a folded or truncated distribution. No attempt was made to work out all the details of a folded Maxwell distribution. However, following the arguments given in johnson and Kotz (1970), the general form for a truncated distribution may be exhibited. This is necessary so that the graphical fitting process described in the sequel can be better appreciated. Johnson and Kotz derivation of a truncated distribution is that for the Gauss distribution. Using the Maxwell p.d.f. given in equation (8), and relabeling f(x;") as z*(x), i.e., by letting " = l:

$$z^*(X) = (4/\%\&B)\, t^2 \exp(-t^2) \quad (9)$$

Using the right-hand side of (9), the cumulative function of the Maxwell distribution can be expressed as:

$$\Phi^*(x) = (4/\sqrt{p}) \int^x t^2 \exp(-t^2) dx \quad (10)$$

Now, following Johnson and Kotz, the truncated Maxwell distribution can be expressed as:

$$f^*(x;a) = \frac{4}{\sqrt{p}} \cdot \frac{1}{a^3} x^2 \exp\left[-\left(x^2 / a^2\right)\right] \left[\frac{4}{\sqrt{p}} \cdot \frac{1}{a^3} \int_A^B t^2 \exp\left[-\left(t^2 / a^2\right] dt\right]^{-1} \quad (11)$$

or expressed as:

$$f^*(x;a) = \left[f_2(a) \right]^{-1} z^*(x) \left\{ \Phi^* \left[\frac{B - f_1(a)}{f_2(a)} \right] - \Phi^* \left[\frac{A - f_1(a)}{f_2(a)} \right] \right\} \qquad (12)$$

where A # x #B - - the lower an~ upper truncation points, respectively $f_1(")$is the E(X), $f_2(") =$ Var(X), $z^*(x)$ and $M^*(x)$ are defined in equation (9) and (lO), respectively. Of course, from equation (12) both the expected value and variance for the truncated Maxwell distribution could be obtained. The M[C] functions in (12), with the truncation points, A and B; are the *degrees of truncation* from below, the A portion, and from above, the B portion [actually (1 - M^* of B)]. If it were known, in the case at hand, that A = E(X), then by replacing B by + 4, the singly-truncated or half-Maxwell distribution would obtain. Since the truncation point A is not known with any reasonable assurance, the graphical fitting process used, essentially, an ad hoc technique to obtain values for $z^*(x)$ and M^* of A. The forgoing disgression was necessary for the presentation of the results.

Figure A-5 shows a graph of the Maxwell distribution in which the left-hand side of the curve--dashed line--is that part of the distribution truncated or which is folded over the right-hand side. The right-hand portion is similar to graphs displayed in the text Figures 3 and 5.

Figures A-6, A-7, A-8 and A-9 display graphs in which the folded-Maxwell distribution was fitted to the azimuth head motion velocities, and to the elevation head motion velocities for Trials 1 and 2, respectively. The middle third of Table A-1 gives the estimates of the parameters used in the graphical fitting process. The lower third of Table A-1 gives the estimates of the parameters to fit the half-normal on half-Gauss distribution. The values used for $z^*(x)$ or M (z) in the table were obtained via trial-and-error using values from a table of the normal distributions during the iterative graphical fitting process. These values appeared to give the "best" fit for the Maxwell and Gauss distributions. If the study would so warrant, further work could be done via some theoretical work to obtain better estimates of values for M (z). Note that for the folded-normal, the value of mode was used as an estimate of the mean. If the value of the truncation point, A, was known with reasonable precision, then that value would have been substituted for ∴ in the Gauss distribution. A better estimate of F also then could have been obtained, if A were known with reasonable precision. Johnson and Kotz (1970) and the references they cite address this particular issue.

DISCUSSION

The results treat the head position and head velocity *as if* these were separate and distinct entities. For that matter, the azimuth and elevation variables are treated in the results as though they are independent of each other. That such is not the case is fairly obvious.

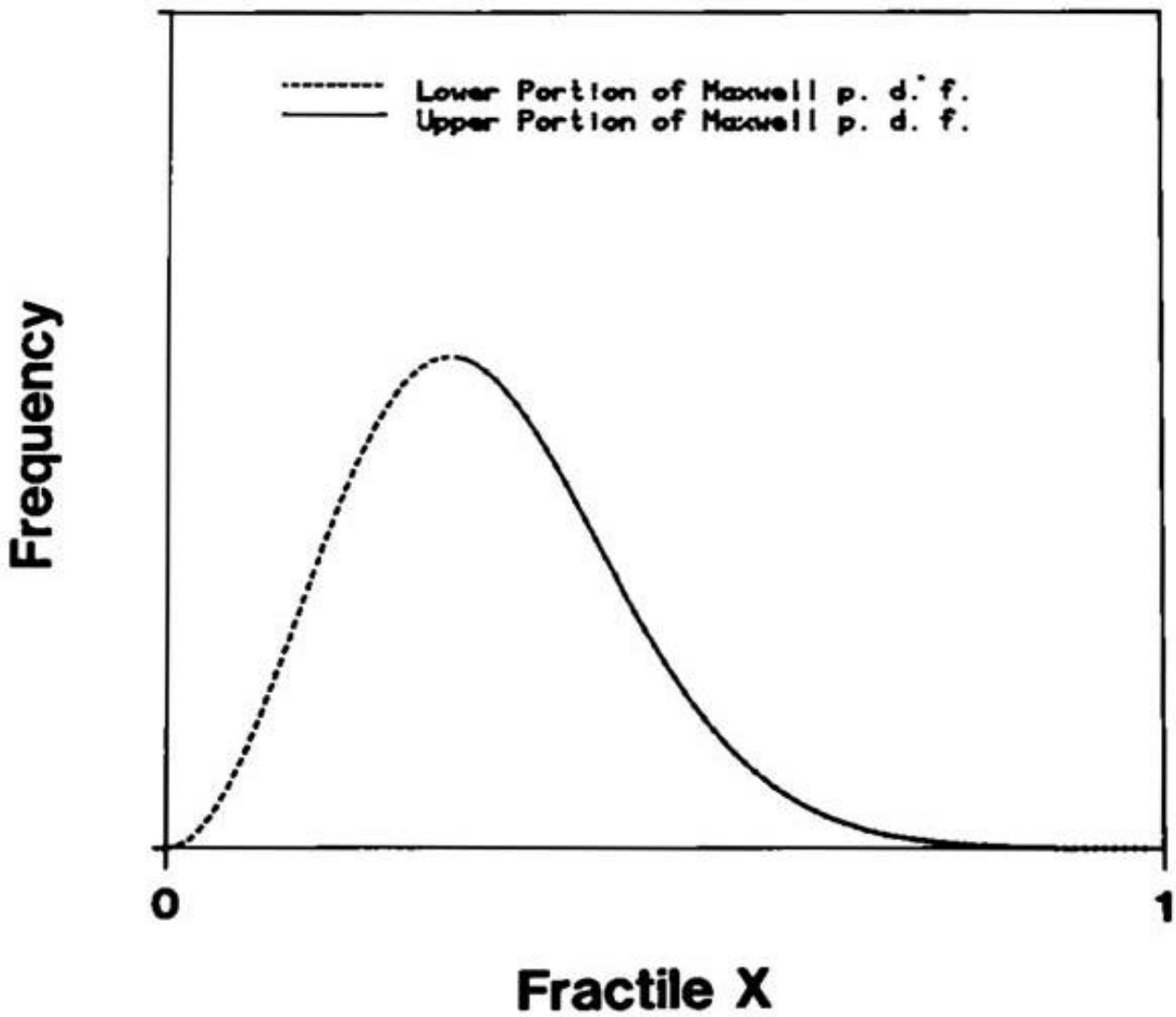

FIGURE A-5. The Maxwell probability distribution function. The dashed part of the curve is that portion folded over the right-hand side–solid line– to produce what is displayed in the velocity histograms given in the text Figures 3 and 5.

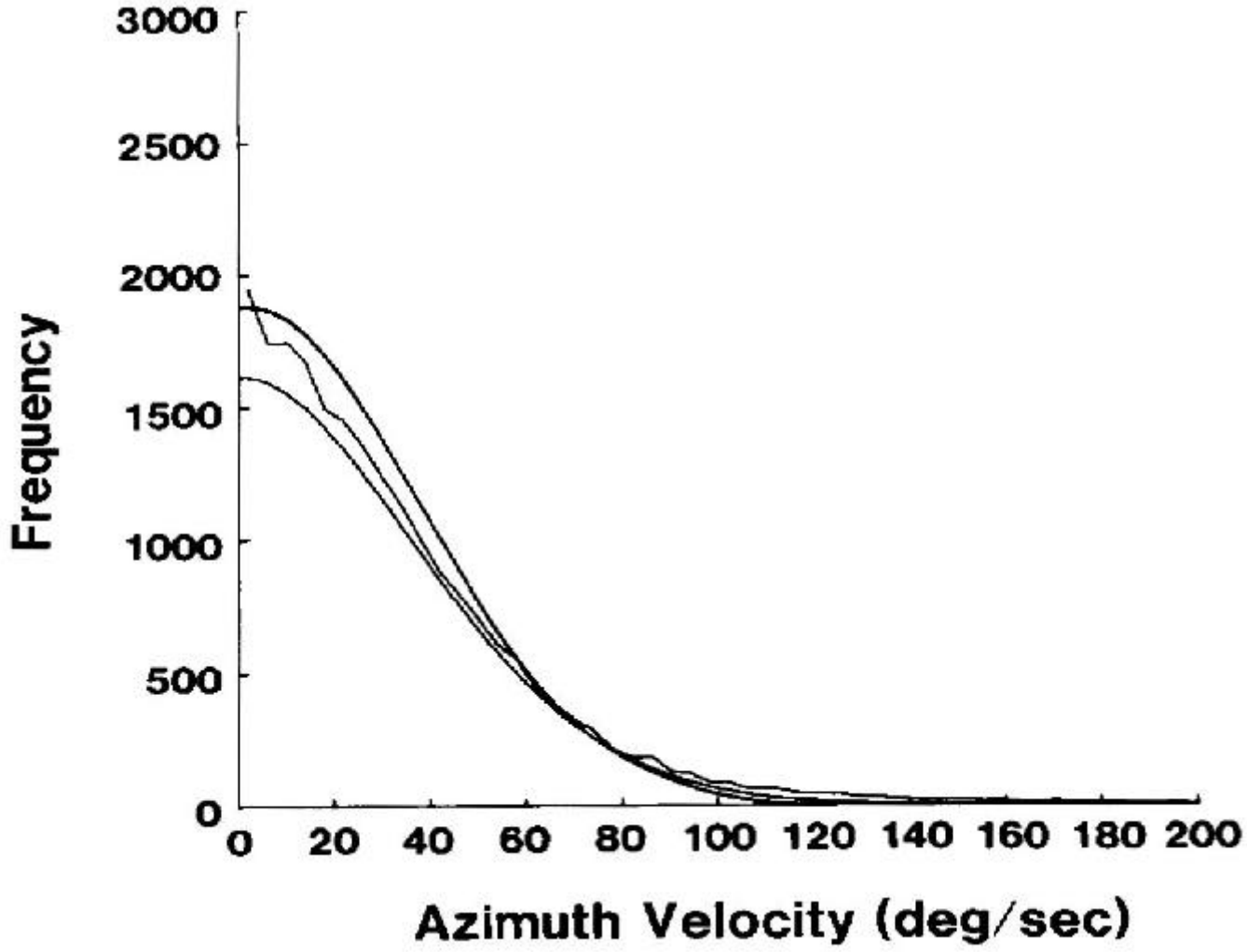

FIGURE A-6. Azimuth velocity of the head frequencies and the fitted Gauss (upper curve) and Maxwell (lower curve) distributions for Subject 3, Trial 1.

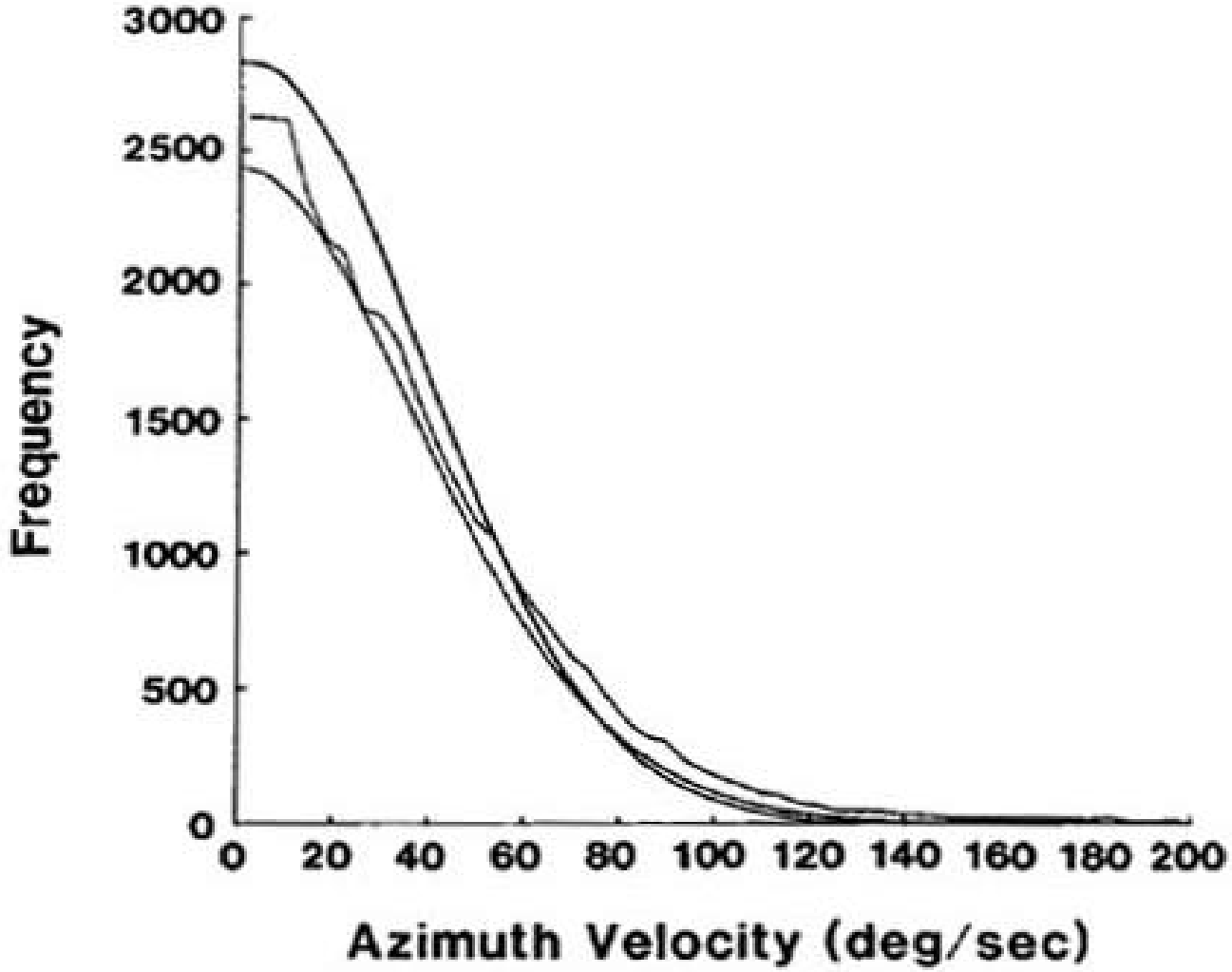

FIGURE A-7. Azimuth velocity of the head frequencies and the fitted Gauss (upper curve) and Maxwell (lower curve) distributions for Subject 3, Trial 2.

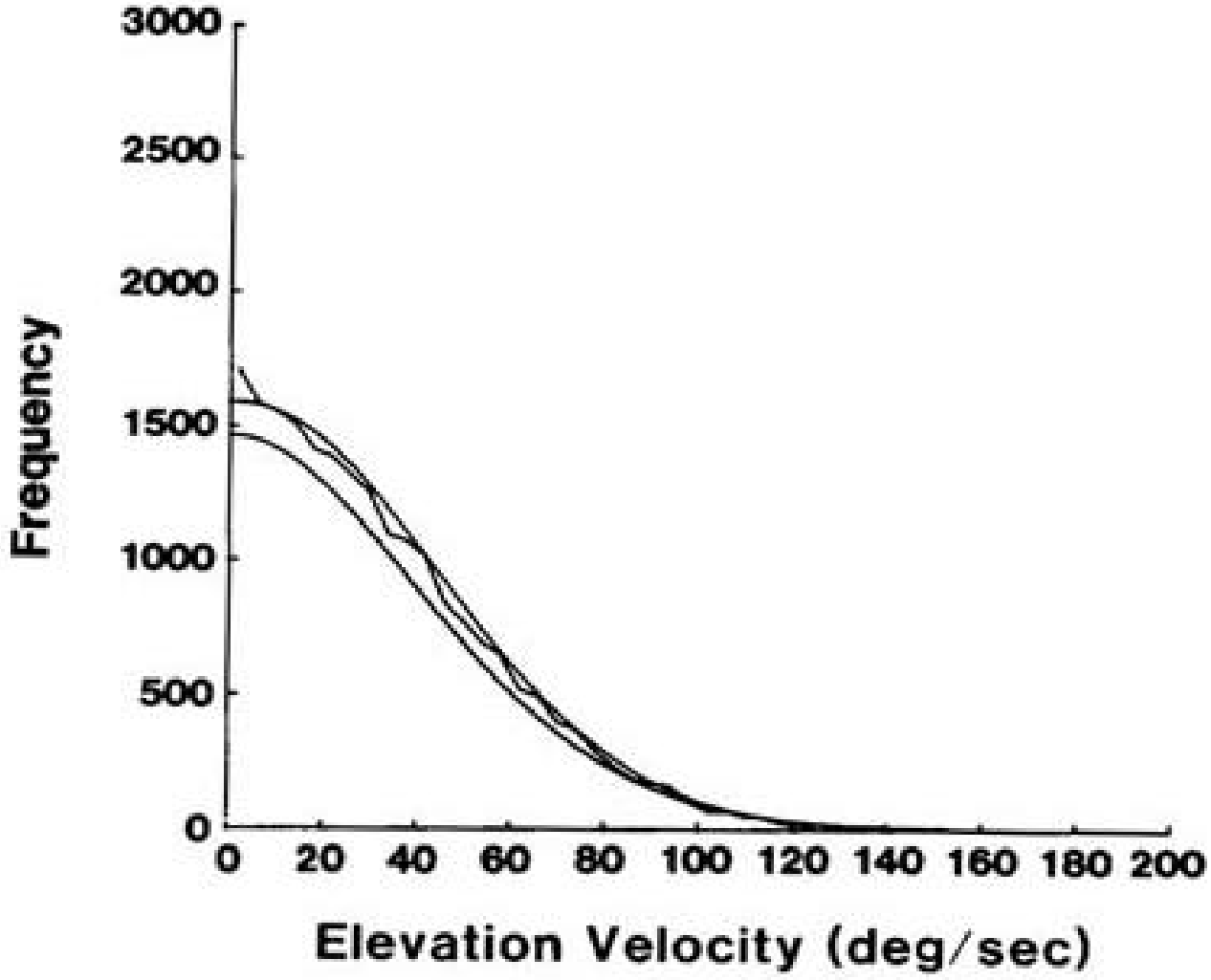

FIGURE A-8. Elevation velocity of the head frequencies and the fitted Gauss (upper curve) and Maxwell (lower curve) distributions for Subject 3, Trial 1.

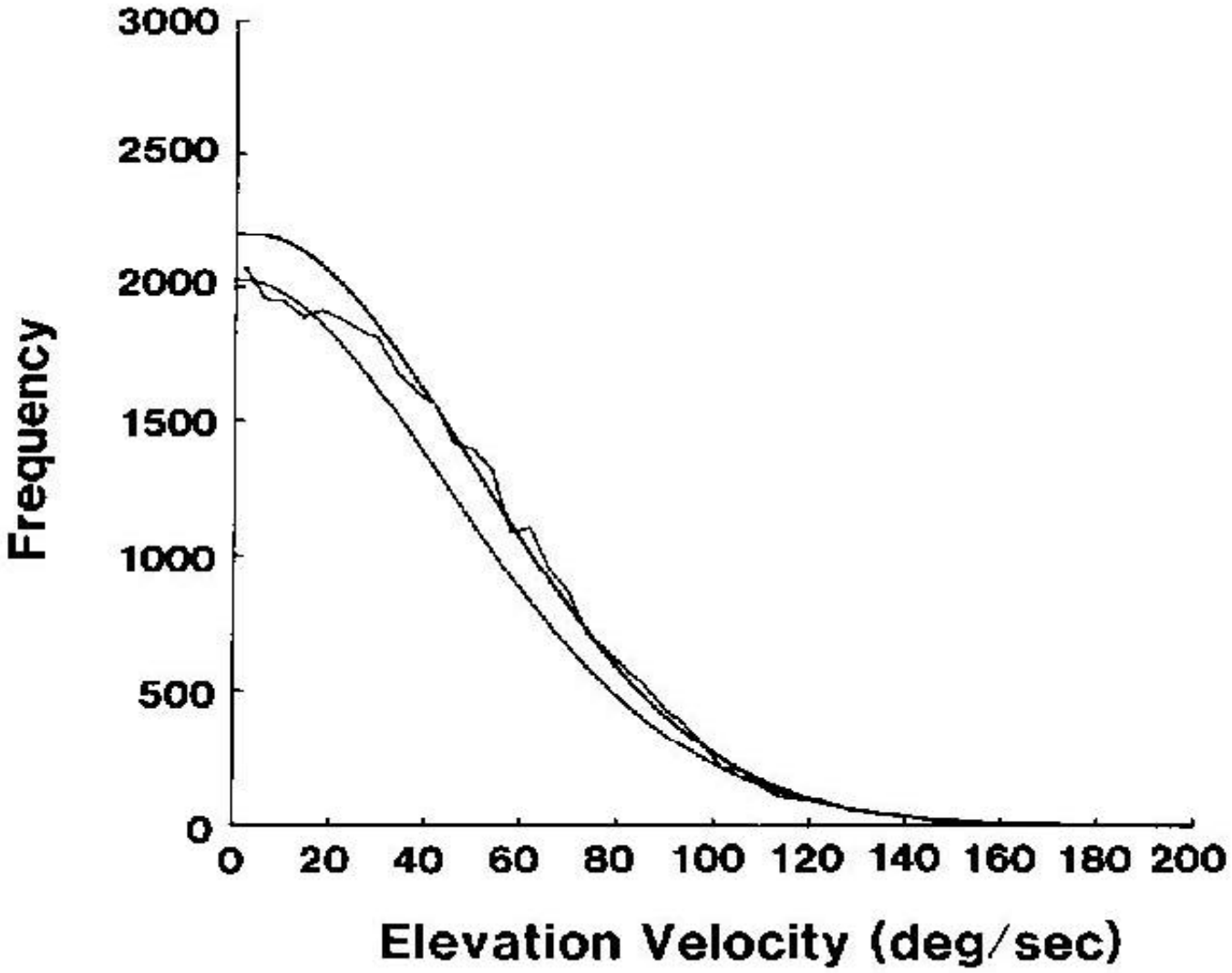

FIGURE A-9. Elevation velocity of the head frequencies and the fitted Gauss (upper curve) and Maxwell (lower curve) distributions for Subject 3.

The motion of the human head as it moves, say, from facing point a to facing point b---change in position--moves at a particular velocity. Moreover, considering the head as a sphere or globe from which a single ray of light emenates and for which a record is kept of its track on a conceptually thin shell or "overhead canopy" is a three-dimensional construct and not a planar one. The three-dimensional aspect of head motion in terms of a stochastic model is discussed in light of the foregoing.

What the histograms of the azimuth and elevation position (text Figures 1 and 2) show are "slices" through a three-dimensional volume. These slices are essentially at right angles to each other. Moreover, the center of each slice--the peak point of each diagram--is the position of the central or main axis of a cone-like object. Since a Cauchy distribution appears to be a reasonable model for both the azimuth and elevation position, at least for subject three's data, a three-dimensional version of a Cauchy distribution can be entertained.

If letting x represent the azimuth position coordinate, letting y represent the elevation coordinate, and letting f(x, y) the frequency of any point in the plane, then the three-dimensional analogue of Cauchy distribution can be written in standard form as:

$$f(x,y) = \frac{1}{2p}\left[1 + x^2 + y^2\right]^{-3/2} \qquad (13)$$

This formula for the three-dimension Cauchy distribution is found in Morgan (1984). Equation (13) can be written in the parametric form as:

$$f(x,y;\, l_x,\, l_{y,} q_x, q_y) = \frac{1}{2p} \cdot \frac{l_x\, l_y}{\left[\left(l_x\, l_y\right)^2 + l_y(x-q_x)^2 + l_x(y-q_y)^2\right]^{3/2}} \qquad (14)$$

where 8_x, 8_y are the shape parameters, and 2_x, 2_y are the location parameters. This function would provide a representation the surface of a structure which has a decidely sharp peak with a steep slope--the steepness depending on either 8_x or 8_y or both--extending outward from the center axis to -4 and $+4$. Note should be made of the fact that a correlation parameter, D, does not appear in equation (13) as it does in the bivariate normal distribution. Johnson and Kotz (1972) mention the three-dimension Cauchy distribution, but they do not give an explicit formula for it.

Returning to the results for the azimuth and elevation position, the graphs shown in Figures A-l, A-2, A-3 and A-4 deserve some comment. First, the fitted curves obviously do not fit the observed data exactly. This is especially noticeable in Figure A-2--Trial 2 of the azimuth position

graph. On the right-hand side of the graph a considerable amount of "noise" in the data is exhibited. In fact, the data appears as if there may exist a second mode in the data. This second mode and a third mode at the left-hand side of the graph are more clearly seen in the text Figure 1. The trimodal aspect of the graph in Figure 1 stems almost entirely from subject four's data. (Figure 1 is the histogram of five subjects' data "lumped together.") Subject four had more experience in searching (from past work in search and rescue missions) than did the other four subjects. Although the graph for subject four's data is not displayed, the histogram for both the azimuth and elevation position of the head is distinctly trimodal with the largest at the center of the histogram. Evidently, subject four's searching strategy was very different from that of the other less experienced subjects insofar as searching is concerned. One conclusion that may be drawn from this observation is that a Cauchy distribution is not an appropriate stochastic model for subjects like subject four. However, the Cauchy distribution may be an appropriate model for subjects who have relatively little experience in searching.

Furthermore, the data for subject three's head position appears to have a "constriction" at the points of inflection of the Cauchy distribution. This may be the result of the fact that the measuring system only permitted measurements of strictly planar motion and it did not permit a direct measurement of the head as it was "tilted" or "canted" during movement. Some of the "noise" depicted in the graphs may be the result of this situation. Of course, other explanations are possible also.

The results for azimuth and elevation velocities suggest that a bi-variate distribution for the head motion velocity could be constructed. If, as the data partially suggests, a Gauss or Normal distribution is an appropriate stochastic model for velocity, then the bivariate Gauss distribution would be appropriate. This distribution is well known to statisticians and others (Johnson and Kotz, 1972), and therefore, will not be discussed further. However, for the velocity bivariate case, if x is the azimuth velocity and y is the elevation velocity, the left-hand portion of the x- and y-axis represents the direction of the head velocity either moving *left* for the azimuth or *down* for the elevation.

The last statement, of course, applies to a bivariate Maxwell distribution. As was pointed out in the results section--the digression on the truncated or folded distribution--the histograms displayed in the text Figures 3 and 5 show the velocity of the head *as if* it were moving in one direction only. Actually, the histograms are a mixture of directional velocities, *i.e.,* to the left and right in the case of the azimuth velocities, and up and down in the case of the elevation velocities.

One salient feature of the histograms displaying the velocity data is that a "shoulder" of sorts ("shoulder of frequencies") appears between the zero frequency and the 15 or 20 degrees/second frequencies. This shoulder appears on all the graphs of velocities for each subject and for each trial. This shoulder, or slight flattening of the frequencies, is more pronounced in some cases than in others. This seemingly peculiar anomaly in the data sets may be a result of the combination of the head motion and eye motion working together. This is to say that at the lower frequencies of velocity the eye movement and the head motion consist of a *coupled system.* Hence, the data

exhibits a certain amount of "noise" at the slower velocities due to the eye movement. This coupled system might be expressed as:

$$\text{Total velocity} = \text{Head velocity (H.V.)} \; r \; \text{Eye velocity (E.V.)} \qquad (15)$$

for $0 < \text{H.V.} < 15$ or 20 deg/sec^2 and the symbol r indicates the coupling funrtion or operator between H.V. and E.V.

The coupling of the head and eyes produces the "shoulder" in the histograms. This shoulder may be one of the reasons that neither the folded-Maxwell distribution nor the folded-Gauss (Normal) distribution fit the data particularly well in this region of the data. Moreover, if only the frequencies of velocities of the eye movement were obtained, then a certain amount of "noise" would be introduced into the eye movement data due to the motion of the head. What is assumed here is that the subject would be searching as the eye movement measurements were being recorded just as was done for the head motion during the search procedure for this study.
The discussion would be incomplete if an attempt was not made to integrate the head position part and head velocity part into some kind of a whole. What follows is such an attempt, but the integration applies soley to those subjects who were less experienced in searching compared to subject four, namely, subjects 1, 3, 5, and 6 only.

The stochastic model which is entertained is that of Brownian Motion (BMO), which derives its name from a Dr. Brown, a botantist, who in the early nineteenth century (circa 1820), observed through a microscope the chaotic-like motion of pollen grains suspended in water. Hence, the name Brownian Motion. Research on BMO continues to this day, but one of the earliest researches done on it which resulted in a definitive mathematical solution was the work of Dr. Albert Einstein, Jr. (Einstein, 1926) at the turn of the twentieth century,

If the mathematical arguments found on page 33 of Durrett's text for BMO (Durrett, 1984) are followed carefully, the Maxwell distribution arises. After some further mathematical developments, he arrives at [his equation (2)]:

$$\Pr_{(x,y)}(B_t = (q,0)) = \frac{\mathbf{y}}{(|\mathbf{x} - q|^2 + \mathbf{y}^2)^{\mathbf{d}/2}} \cdot \frac{\Gamma(\mathbf{d}/2)}{{}_p\mathbf{d}/2} \qquad (16)$$

where B_J is the motion, 2 is a parameter, x and y are the coordinates of the system, and d is the "dimensionality" of the process. Equation (15) can be recognized as the three-dimension analogue of the Cauchy distribution given in equations (13) and (14). For equation (16) d is set equal to three, of course, to obtain equation (14). Moreover, Durrett calls the equation (16) *a Cauchy Process.*

Durrett's development implies that the position of a particle can be obtained via the Maxwell distribution and the paper by Doob (1942) implies essentially the same thing. Thus a stochastic model for the head motion of an aviator while searching (relatively inexperienced pilots with respect to searching only) may be likened to BMO in three dimensions. However, there exists one important difference between the motion of the head and the motion of a particle. The BMO of a particle is a result of external forces while the motion of the human head is the result of "internal forces." The "internal forces" for a human is, of course, the mind-body system
.

The observed position frequency distributions for subject four are very different from the observed frequencies for the other subjects. This suggests that the mind-body system can or could be trained to adopt a different searching strategy than the one employed by the relatively inexperienced searchers in this study. Moreover, from a modeling view point, the distribution of the head position for the "ideal" searcher/pilot would, in the limit, be that of a bivariate uniform distribution, i.e.:

$$f(u,v)=(1-a)\left[(2uv-u-v)a+1\right]y(u,v)^{-3/2}$$
$$where\ y(u,v)=\left[a(u+v)=1\right]^2+4a(1-a)uv \qquad (17)$$
$$and\ a\le 1, 0\le u,v\le 1. (Morgan, 1984).$$

The bivariate uniform distribution is envisioned since, going in a "backward" direction, the Cauchy distribution can be generated from the ratio of two unit Normal distributions each of which can be generated from a uniform distribution. In a practical sense, the human pilot should be able to reverse this process via appropriate changes in searching strategy.

The trimodal aspect of subject four's head position frequency data as well as the much less pronounced tri- or bimodality of the other four subjects' head position frequencies suggests that these data are actually a mixture of at least two and probably three distributions. Mixtures of distributions are a large problem into which research is actively being done. The disentangling of mixtures of distributions is difficult and time consuming work. This data for this particular study did not warrant the effort in view of the fact that only one subject (a sample of size one) exhibited a pronounced mixing of distributions. -This would preclue, of course, any inferences to be made to a polulation of aviators. However, the interested reader can pursue this topic in Everitt and Hand's 1981 text. Moreover, a mixture of three distributions should not be a surprising feature of the data for at least two reasons. Human being, generally, turn their head left and right while engaged in any work involving forward movement of the whole body. In this case, the forward motion is the motion of the aircraft. The natural tendency is to look and face forward. However, there also exists the tendency to face, even momentarily, left or right, as progress is made in the forward direction, i.e., the human does not stare or gaze directly ahead all the time. The amount of time spent with the head facing left or right will govern the generation of additional distributions within a set of frequencies.

If the reader has persevered this far, a natural question will, no doubt, have arisen in the reader's mind. The question may be: "Of what particular value or what practicable application does all this have"? The following example may provide an answer to this question.

Suppose the question is posed: What is the probability that an aviator will, while searching, be looking between the points b_1 and b_2? (The example is applied to the azimuth position of the head only.) If the assumption is made that 2_2 in equation (2) is equal to 6.727 degrees or 0.117 radians and 2_1 is set equal to zero, then the probability that the aviator is searching between points b_1 and b_2 is found by:

$$\Pr(b_1 \le x \le b_2) = \frac{1}{p} \int_{b_2}^{b_1} \frac{\mathbf{0.117}}{(\mathbf{0.117})^2 + (\mathbf{x})^2}\,\mathbf{dx} \tag{18}$$

which reduces to:

$$\Pr(b_1 \le x \le b_2) = \frac{1}{p}\left[\tan^{-1}\left(\frac{b_2}{0.117}\right) - \tan^{-1}\left(\frac{b_1}{0.117}\right)\right]. \tag{19}$$

If, say b_1 = 0 degrees and b_2 = 20 degrees (b_1 = 0 radians and b_2 = 0.349 radians), then, using equation (19), Pr(0#x#20) : 0.487, approximately. In a similar manner, the probability of the head velocity may be obtained for two points or the probability may be obtained that the head velocity will be greater than, say k degrees/second by using the folded-Maxwell distribution or folded-Gauss distribution.

SUMMARY

The purpose of Appendix A is to construct a stochastic (probability) model of the head motion of helicopter aviators while they were engaged during flight in searching for another helicopter in flight. The data from five subject pilots were used as a basis for building the model. These data consisted of the frequencies of azimuth and elevation head position and the frequencies of azimuth and elevation head velocities for each pilot. These frequencies were obtained from time series measurements. The time series (flight time) were between 20- and 30-minutes duration or about 2400 to 3600 total measurements of the head position and velocity for each trial or run. These were processed via a computer program so as to provide frequencies of the head position measured in degrees and frequencies of head velocity measured in degrees/second.

Two methods were used in constructing the stochastic model, i.e., probability distribution function (p.d.f.). First, the modeling was guided by the frequency diagrams and the summary statistics; second, the modeling was done using elements from mathematical statistics. A constraint imposed on mathematical statistics required that the mathematical model, i.e., p.d.f., provide a reasonable model or a sensible one.

The results of the modeling effort are:

1. A Cauchy p.d.f, is a reasonable model for both the azimuth and elevation positions of the head.
2. Two competing models for the head velocity, which are reasonable models of both azimuth and elevation velocity of an aviator's head are:

   a. The folded Maxwell p.d.f.

   b. The folded Gauss (Normal) p.d.f.

The folded Maxwell p.d.f, is possibly the preferred model for the head velocity since the Maxwell p.d.f, is a model for the velocity of gas molecules. From a pragmatic point of view, either the Gauss or the Maxwell p.d.f, are candidates for a stochastic model of head velocity.

The models cited apply only to the data from four subjects' trials (each subject pilot did two trials or runs)*. These subjects had relatively little experience in searching. Subject number four's position data were very different from the other four subjects' in that his head position data, especially the azimuth position data, were trimodal. Subject four had considerably more searching experience. The pronounced trimodality of his data

* Subject three data are depicted in Appendix A. The combined daLa for the five subjects are depicted in the body the text.

suggests that the data set is a mixture of at least three p.d.f.'s. No attempt was made to construct a stochastic model which would embody a mixture of p.d.f.'s.

Although an attempt was not made to construct a detailed model which would encompass the three dimensional aspect of head motion, a "synthesis" of the two dimensional results proffers a three-dimensional analog (bivariate) of Cauchy p.d.f, as a model for the head position. The synthesis shows also that either a bivariate Gauss p.d.f, or a bivariate Maxwell p.d.f, can be regarded as a suitable model for head velocity in three dimensions.

Further synthesis - assuming that the bivariate models hold - proffers the idea that head motion of an aviator while he is searching is analogous to Brownian Motion (BMO) in three dimensions. The BMO in three dimensions incorporates both the position of the head motion and velocity of the head motion. This general model applies only to those aviators with a minimal amount of searching experience.

A "shoulder of frequencies" in the diagrams of the velocity frequencies appears between the zero frequency and the 15 or 20 degrees/second^2 frequencies. This seemingly peculiar anomaly in all the velocity data sets suggests that what is being measured at the lower frequencies is a combination of both head velocity and the eyes' movement velocity. This combination is termed a *coupled system, i.e.*, a coupling of the head motion with that of the eyes' motion.

The usefulness of the models is illustrated with an example of the calculation of the probability that the head position will be between points b_i and b_2 using the Cauchy p.d.f, applied to azimuth position. Similar probability calcuations can be done using either the folded Maxwell p.d.f, or the folded Gauss p.d.f, applied to head velocity.

APPENDIX B

A Note on the Derivation of the First Four Moments and Measures of Skewness, $\$_1$, and Kurtosis, $\$_2$, of the Maxwell Probability Distribution Function.

INTRODUCTION

The Maxwell probability distribution function (p.d.f.) provides a stochastic model of the velocity of gas molecules, i.e., probability model. Dr. James Clerk Maxwell in his paper "On the Dynamical Theory of Gases" published in 1866 *(Philosophical Transactions* Vol. 157) derived this p.d.f. based on theoretical considerations alone. A reprint of Maxwell's 1866 paper is found in Niven (1965). Not until 1920 was Maxwell's theoretical development verified by direct measurements. More precise measurements which verified the correctness of the theory were not made until 1947 (Sears and Zemansky, 1963). On page 462 of their text is a figure in which is depicted a graph that shows the remarkable agreement between the experimental results of the measurements gas molecule velocities and Maxwell's model derived nearly 80 years before such an experiment was done.

The Maxwell p.d.f. can be written as a differential equation:

$$\frac{dN}{dV}=\frac{4N}{\sqrt{p}}\left(\frac{m}{2KT}\right)^{3/2} v^2 \exp\left[-\left(mv^2/2KT\right)\right] \qquad (1)$$

where N is the number of gas molecules, m is the mass of a molecule, T is absolute temperature, v is the velocity o-f the molecules (Maxwell's derivation expressed v as a vector of the three direction components of velocity), K is the Boltzmann-Maxwell constant*, and the constants B and exp(=e) have their usual mathematical definitions. If the term m/2KT is set equal to β^2, equation (1) can be expressed as:

$$f(x;s)=\begin{cases} \dfrac{2s^3}{\sqrt{2p}} \quad x^2 \exp\left[-\left(x^2 s^2/2\right)\right]; x \geq 0, s > 0 \\ 0, elsewhere \end{cases} \qquad (2)$$

* According to Menzel (1960) the Boltzmann~s constant--sometimes called the Maxwell-Boltzmann constant--has the following value:

K = 1.38044 $\pm$ 0.00007 x 10^{-16} erg/deg.

where x = v, the velocity. Equation (2) is the p.d.f, given by Tsokos (1972). Parzen (1960) expresses the Maxwell p.d.f, in a similar but not identical fashion as Tsokos' formula:

$$f(x;a) = \begin{cases} \frac{4}{\sqrt{p}} \frac{1}{a^3} x^2 \exp[-(x^2 / a^2)]; x \geq 0, a \geq 0 \\ 0, \text{elsewhere} \end{cases} \quad (3)$$

where x= v, the velocity and the parameter, ", is equal to / 2/F -- F is the parameter in equation (2).

Although Tsokos gives the expected value, E(X), *i.e.*, first moment, the Var (X), and $_1, a measure of skewness, neither Tsokos nor Parzen provide or give a summary of the first four ordinary moments and the formulae for both $_1 and $_2. A review of available statistical literature did not reveal the estimators for these statistics.

The purpose of this note is to give the derivation of the moments and measures of skewness and kurtosis, a summary of these results using Tsokos' and Parzen's p.d.f, formulae, and a discussion of the results with a comparison of the Maxwell p.d.f, with that of the Gauss p.d.f.--the so-called normal density distribution.

METHODS

The methods used to find the moments of a probability distribution function, p.d.f., of a random variable X are fairly well-known by statisticians. (The p.d.f, will be called simply the distribution throughout the sequel.) Both Tsokos' and Parzen's texts, as well as many other texts on mathematical statistics, give an introduction to these methods. The method can be summarized in the following way.

Given a random variable X with a distribution f(x), where f(x) is continuous and bounded, the k^{th} moment or k^{th} ordinary moment of the variate X is given by:

$$m_k = E(X^k) = \int_{-\infty}^{\infty} X^k f(x)\,dx; k = 1,2,\ldots \quad (4)$$

and assuming that the integral converqes.

The k[th] moment of f(x), with respect to any point b, is given by:

$$E\left[(X-b)^k\right]=\int_{-\infty}^{\infty}(x-q)^k f(x)dx; k=1,2,\ldots \quad (5)$$

where E[@] denotes the expected value about the point. The k[th] moment of f(x), with respect to E(X) =2,

$$h_k = E\left[(X - E(X)\right]^k = \int_{-\infty}^{\infty} (x-q)^k f(x)dx; K-1,2,\ldots \quad (6)$$

where 0_k is called the k[th] central moment of X. The first four central moments can be found from the ordinary moments from the following equations:

$$h_2 = m_2 - m_1^2, for\ k = 2 \quad (7)$$

$$h_3 = m_3 - 3m_1m_2 + 2m_1^3,\ for\ \ k = 3 \quad (8)$$

$$h_4 = m_4 - 4m_1m_3 + 6m_1^2m_2 - 3m_1^4,\ for\ k = 4 \quad (9)$$

where 0_2 is the variance of a distribution and the positive square root of 0_2 is known as the standard deviation.

The characteristic function and the moment generating function can also be used to find the moments and expected values for a distribution. Tsokos gives the characteristic function and moment generating function for the Maxwell distribution. The characteristic function is:

$$f(t) = \frac{e - t^2 / 2s^2}{\sqrt{2p}\ s^2} \quad (10)$$

The moment generating function is:

$$m(t) = \frac{e^{t^2/2s^2}}{\sqrt{2p}\,s^2} \tag{11}$$

These functions will not be used in the sequel to obtain the first four central moments of the Maxwell distribution.

Since the random variable X is considered a velocity, the integrals in equations (4), (5), and (6) are bounded from below by zero, ~.g., the integral in equation (4) must be written as

$$\int_0^\infty x^k f(x)dx.$$

To evaluate the odd kth ordinary moments the integral, which is found in the 26th edition (1981) of "Standard Mathematical Tables" edited by W. H. Beger, the CRC Press (Boca Raton, FL) on page 342--integral number 667, is used. This integral is:

$$I_1 = \int_0^\infty x^{2n+1} e^{-ax^2} dx = \frac{n!}{2a^{n+1}}; (a > 0). \tag{12}$$

To find the even k[th] ordinary moments, the following integral (number 666 on page 342 of the CRC Tables) is used:

$$I_2 = \int_0^\infty x^{2n} e^{-ax^2} dx = \frac{1 \bullet 3 \bullet 5 \ldots (2n-1)}{2^{n+1} a^n} \sqrt{p/a} \tag{13}$$

where a > o.

Once the first four central moments of a distribution are calculated, the measure of skewness, β_1, and kurtosis, β_2, are easily found using the following formulae:

$$b_1 = n_3^2 / n_3^2 \tag{14}$$

$$b_2 = n_4 / n_2^2 \tag{15}$$

The Pearson measure of skewness, which is applicable to a wide class of frequency-distributions, uses both β_1 and β_2 :

$$Sk = \frac{\sqrt{b_1(b_2+3)}}{2(5b_2 - 6b_1 - 9)} \tag{16}$$

The reader should note that in some statistical computer programs, β_1 and β_2 are expressed as Y_1 and Y_2 (or g_1 and g_2) where

$$Y_1 = \beta_1 \tag{17}$$

and

$$Y_2 = \beta_1 - 3 . \tag{18}$$

For the Gauss distribution, $Y_1 = \beta_1 = 0$ and $\beta_2 = 3$ or $Y_2 = 0$. These values sometimes are used to assess whether or not an observed or empirical distribution is or is not a Gauss or Normal distribution. However, the estimates for these statistics must be based on fairly large samples and both statistics are sensitive to outliers or aberrant values.

RESULTS

To obtain the first and third ordinary moments use is made of I_1, equation (12). The first moment or mean is found, using Parzen's formula, by setting:

$$E(X) = m_1 = \frac{4}{\sqrt{p}} \bullet \frac{1}{a^3} \int_0^{\infty} \times x^2 \exp[-(x^2 / a^2)] dx \qquad (19)$$

Letting 2n + 1 = 3 which implies that n = 1 and setting a = 1/"^{2}, then

$$m_1 = \frac{4}{\sqrt{p}} \bullet \frac{1}{a^3} \left[\frac{1!}{2(1/a^2)^2} \right] \qquad (20)$$

Then, after some algebra,

$$m_1 = 2a / \sqrt{p} \qquad (21)$$

Since the parameter, F, in Tsokos' f(x) is equal to $\sqrt{2} / a$, substitution in equation (21) yields

$$m_1 = 4 / s\sqrt{2p} \qquad (22)$$

for the first moment or E(X) for Tsokos' expression of the Maxwell distribution.

In a like manner, i.e., using I_1 again, the third ordinary moment is found, namely:

$$E(X^3) = m_3 = 4a^3 / \sqrt{p} \qquad (23)$$

In terms of Tsokos' parameter, F,

$$E(X^3) = m^3 = 16 / s^3\sqrt{2p} \qquad (24)$$

To find the even ordinary moments, namely, $E(X^2)$ and $E(X^4)$, use is made of the integral I^2 in equation (13). $E(X^2)$ is found, then, by:

$$E(X^2) = m_2 = \frac{4}{\sqrt{p}} \bullet \frac{1}{a^3} \int_0^{\infty} x^2 \, x^2 \exp\left[-(x^2 / a^2)\right] dx \qquad (25)$$

Letting 2n = 4 which implies that n = 2 and setting a = 1/"^{2}, then

$$m_2 = \frac{4}{\sqrt{p}} \bullet \frac{1}{a^3} \left[\frac{3!}{2^3 (1/a^2)^3} \sqrt{p / a^2} \right] \qquad (26)$$

after doing the algebra,

$$:_2 = 3"^2 / 2 \qquad (27)$$

or, in terms of F,

$$:_2 = 3/F^2 \qquad (28)$$

In a similar fashion, i.e., using 12 again, the fourth ordinary moment is found to be:

$$E(X^4) = :_4 = 15"^4 / 4 \qquad (29)$$

or in terms of F,

$$u_4 = 15/F^4 . \qquad (30)$$

The first four central moments, *i.e.*, moments around the mean or E(X), substitution of the first four ordinary moments, $:_1$, $:_2$, $:_3$, and $:_4$ into the formulae given in equations (7), (8) and (9) is done. Of course, the first ordinary moment and the first central moment, n~, are identically equal.
Making the required substitution followed by appropriate algebraic manipulation, the following are obtained:

$$n_1 = E(X) = 2" / \%\&B \qquad (31)$$

$$n_2 = "^2 (3/2 - 4/B). \qquad (32)$$

$n_3 = \alpha^3 [(16 - 5\beta) / \beta\gamma\beta]$ (33)

$n_4 = \alpha^4 (15/4 + 4/\beta - 48 / \beta^2)$. (34)

Using $\gamma = \gamma\beta/\alpha$ as done previously, the n_i, i = 1, 2, 3, 4, can be expressed in terms of the parameter γ.

To obtain the expression for δ_1 and δ_2, substitution of the appropriate n_i s into equations (14) and (15) is done. The substitutions followed by some tedious algebra yields:

$\delta_1 = [8 (16 - 15\beta)^2 / (3\beta - 8)^3]$ (35)

and

$\delta_2 = [\beta(15\beta + 16) - 192] / (3\beta - 8)^2$ (36)

Tsokos' formula for δ_1 which he denotes as θ is:

$\delta_1 = \theta = [2\sqrt{2}(16 - 5\beta)] / (3\beta - 8)^{3/2}$. (37)

Numerical values can be obtained for δ_1 and δ_2 since the parameter α (or γ) is not contained in equations (35) or (36). These estimates are:

$\hat{\delta}_1 = 0.235898...$

and

$\hat{\delta}_2 = 3.10816...$.

The estimates obtained for B1 and Be were verified using numerical integration. A computer program written in BASIC for a micro-computer was used. The numerical integration technique was a modified version of the Newton-Cotes quadrature method. The numerical analysis computation gives an assurance of the correctness of the derivation of the moments and measures of skewness, δ_1 and kurtosis, δ_2.

The results of the foregoing derivations are summarized in Table B-1.

DISCUSSION

The Maxwell distribution is a member of the family of exponential distributions. The Gauss or Normal distribution is also a member of this family. The Gauss distribution can be written as:

$$f(x;\, m,\, s) = \frac{1}{s\sqrt{2p}}\, x^{s}\, \exp\left[-(x-m)^2 / 2s^2\right] \qquad (38)$$

where the parameter : and F are the population mean and standard deviation, respectively. Equation (38) was deliberately written with the term x^0. The value of x^0 is, of course, equal to one. This shows that the Maxwell distribution and the Gauss distribution are "cousins" in the family of exponential distribution. In fact, their graphs appear, at first glance, to be nearly identical. However, the Gauss distribution differs from the Maxwell distribution in certain ways other than the obvious one, *i.e.,* it has x^2 in it.

The Gauss distribution is a two parameter distribution in which : is the location parameter and F is the shape parameter. On the other hand, the Maxwell distribution has but one parameter which plays the role of both the location and shape parameter. Moreover, the Maxwell distribution is bounded from below by zero, i.e., the x-values must be zero or positive real numbers, while the x-values for the Gauss distribution have the range -% to +%. The fact that the x-values for Maxwell distribution must all be positive numbers is not surprising since velocities are positive entities. Velocities may, however, have either a positive or negative direction depending on the reference frame, but velocities of themselves are positive quantities. A zero velocity is merely a means of saying that a body or object is at rest, *i.e.,* not moving.

Parzen indicates that the Maxwell distribution can be derived from the x-distribution is (N.B. This is not the chi-squared distribution!):

$$f(x;n,\ ) = \begin{cases} \dfrac{2(n/2)^{n/2}}{s^{\,n}\Gamma(n/2)}\ x^{n-1}\exp[-(n/2s^2)]\,x^2, n = 1,2,\ldots, and\ s > 0 \\ 0, elsewhere \end{cases} \qquad (39)$$

Parzen says that the Maxwell distribution can be derived from equation (39) by letting n = 3 and F = " %&2. If this is done and recalling that $(3/2)^{312} = 1$ and ' (3/2 = %&/2, then the Maxwell distribution obtains after some simple algebra.

TABLE B-1
SUMMARY OF THE FIRST FOUR MOMENTS AND ESTIMATORS OF THE MEASURES OF SKEWNESS, β_1 AND KURTOSIS, β_2, FOR THE MAXWELL PROBABILITY DISTRIBUTION FUNCTION (P.D.F)

Function form and Estimators	Parzen's	Tsokos'	Notes
f(x; θ)	$\frac{4}{\pi}\ \frac{1}{\alpha^3}\ x^2\ \exp[-(x^2/\alpha^2)]$	$\frac{2s^3}{\sqrt{2\pi}}\ x^2 \exp\left[-(x^2 s^2/2)\right]$	θ is: $\theta = \pi/\alpha$
Expected Values:			
E[x]	$2\alpha/\pi$	$4/\theta\pi$	
$E[x^2]$	$3\alpha^2/2$	$3/\theta^2$	
$E[x^3]$	$4\alpha^3/\pi$	$16/\theta^3\pi$	
$E[x^4]$	$15\alpha^4/4$	$15/\theta^4$	
Moments around θ:			
n:	$2\alpha/\pi$	$4/\theta\pi$	
n^2	$\alpha^2(3/2 - 4/\pi)$	$(2/\theta^2)(3 - 4/\pi)$	
n^3	$\alpha^3[(16 - 5\pi)/\pi\sqrt{\pi}]$	$(2\sqrt{2}/\theta^3)[(16 - 5\pi)/\pi\sqrt{\pi}]$	
n^4	$\alpha^4(15/4 + 4/\pi - 48/\pi^2)$	$(1/\theta^4)(15 + 16/\pi - 192/\pi^2)$	
β_1, skewness	$[8(16 - 15\pi)^2/(3\pi - 8)^3]$	$Y = [2\sqrt{2}(16 - 5\pi)]/(3\pi - 8)^{3/2}$	Approximate values: 0.235898
β_2, kurtosis	$[\pi(15\pi + 16) - 192]/(3\pi - 8)^2$	(Same as Parzin's)	3.10816
References	Parzen, E. 1960 Modern Probability Theory and Its Applications.. NY: John Wiley & Sons, Inc	Toskos, C. P. 1972. Probability Distributions: An Introduction to Probability Theory with Applications. Belmont, CA: Duxbury press.	

To obtain estimates of either the parameter α or σ in the Maxwell distribution the method of moments can be used. If s_x is calculated or an estimate of the standard deviation σ is calculated from a sample of size n - - where n is assumed to be large - - then, from Table B-l,

$$s_x = 2\alpha / \sqrt{3} \qquad (40)$$

or

$$\sigma^2 = \alpha^2 (3/2 - 4/\pi) \qquad (41)$$

solving for α in either equation yields an estimate of α.

A theoretical feature of the Maxwell distribution is that it arises in consideration of and theory of Brownian Motion (BMO). Doob (1942) mentions that the Maxwell distribution is obtained in the limit (as t, time, approaches ∞) of a temporally homogeneous differential stochastic process the distribution of which is Gaussian with mean 0, variance $\alpha^2 |t|$ and with mutually independent chance (random) variables. Wang and Uhlenbeck (1945) mention that the work of Dr. N. Wiener on the theory of BMO started with the Maxwell-Bolzmann distribution (Maxwell distribution) law of velocities of gas molecules. Both the papers by Doob, and by Wang and Uhlenbeck are found in Wax (1954). Durrett's recent text (Durrett, 1984) does not cite the Maxwell distribution explicitly, but nonetheless, some of his mathematical arguments imply that the velocity distribution (not displacement) in BMO is subassumed to follow the Maxwell distribution. Durrett also refers to Doob's 1942 paper. Feller (1971) also cites the Maxwell distribution in connection with BMO. The main point to be made from these particular references is that the Gauss distribution and Maxwell distribution are related to each other via consideration of BMO. For that matter, the mean, u, and the standard deviations σ, in the Gauss distribution differ from the Maxwell distribution only by a multiplicative constant--the constant is different for the two parameters in the Gauss distribution.

The difference between these two distributions are illustrated in Figure B-1. The graph shows the Maxwell distribution depicted as a solid line while the Gauss distribution is shown as a dashed line or curve. The graph of the Maxwell distribution shows that it is skewed with a long tail extending in the right-hand direction while the Gauss curve is symmetric, but a portion of the left-hand tail takes on negative values. The fact that the Maxwell distribution is "more peaked" than that of the Gauss on~ can not be as well discerned in Figure B-1 as the skewness of the Maxwell density can be discerned. This is not surprising since the value of β_2 - - measure of kurtosis - - for the Gauss distribution is equal to 3, but the value of β_2 for the Maxwell one is approximately 3.108 which is only about a 3.6 percent difference from 3.

A natural question is what difference or consequence, if any, would obtain if, for a statistical analysis of velocities, say, the Gauss or Normal distribution was assumed instead of the Maxwell distribution 'For reasonably large samples (the matter of sample size to be discussed later in the sequel), very little difference if any would result. However, for small or moderate sample sizes, the difference in assuming the Gauss distribution over that of the Maxwell one could be substantial insofar as the fnferential process is concerned. This stems from the fact that if a sample of velocities is made from a Maxwell distribution, then one to several of the measurements might appear to be

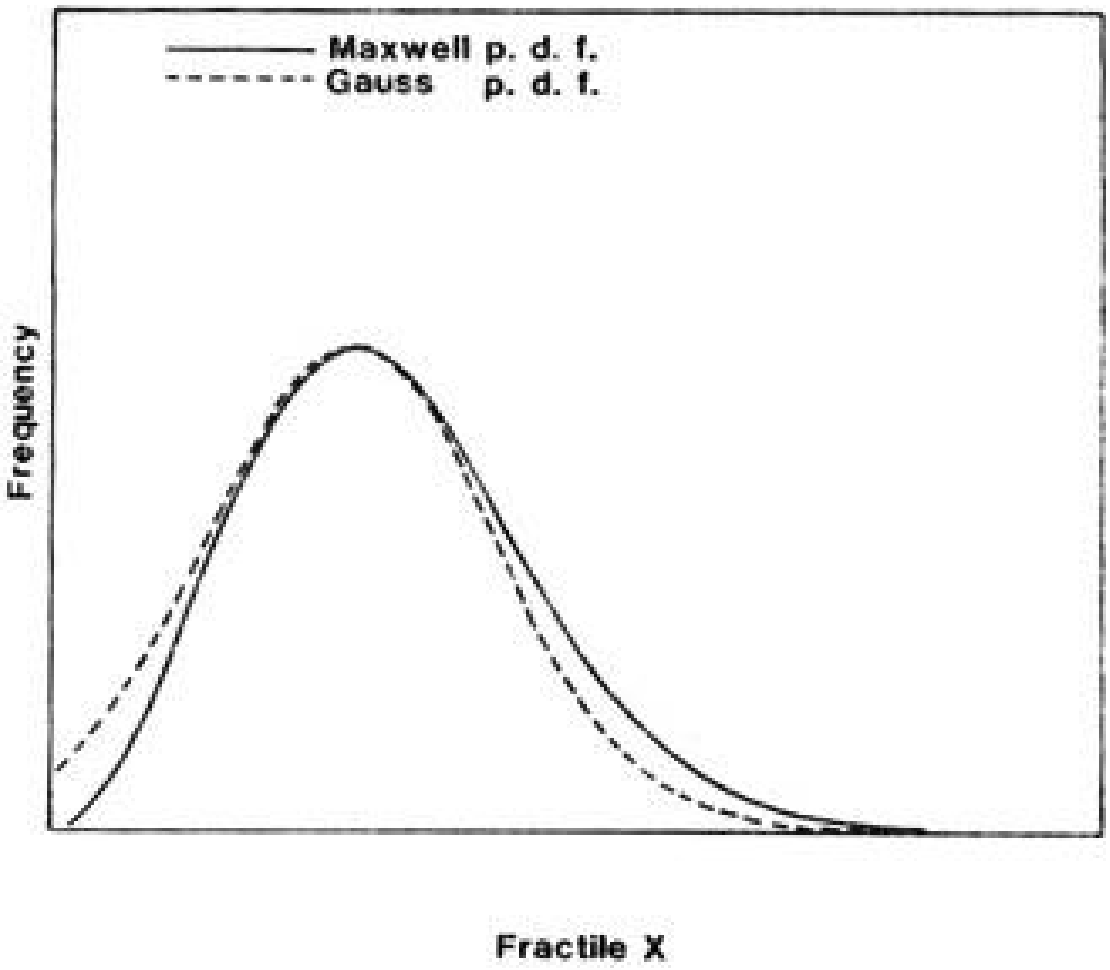

Figure B-1. The Maxwell probability distribution function (solid line curve) and the Gauss on so-called Normal probability distribution function (dashed line curve). The Maxwell distribution is skewed as compared to the Gauss distribution which is symmetric. The Maxwell distribution is slightly more "peaked" - - the kurtosis, as measured by β_1, is positive - - compared to the Gauss distribution.

outliers when they are actually values from the long right-hand tail of the Maxwell distribution. Although statisticians have recommended using the reciprocal of velocity measurements in, for example, the analysis of variance, transforming the velocity measurements via the method given by Bartlett (1947) is suggested. Further details of this technique are given by Kendall and Stuart (1966).

The essence of Bartlett's technique is that given the variance of distribution expressed as a function of the mean or expected value, a variance-sta-bilizing tranfnrmation may be obtained from (using Bartlett's notation):

$$g(m) = \int \frac{C\,dm}{\sqrt{f(m)}} \tag{42}$$

where F_X^2 = f(m) and m is the mean of x.

Using the results given in Table B-l, substituting E(X) into the Var(X) for Parzen's formulation, and evaluating the indefinite integral given in equation (42), the following obtains:

$$g(m) = \frac{1}{\sqrt{a}} 1n(x) \tag{43}$$

where a is a constant and the value of 1 / %6 is approximately 1.8311. Thus, if the assumption is made that the underlying distribution is a Maxwell one, then equation (43) could be used to stabilize the variance for a particular statistical analysis.

The matter of sample size has been mentioned. In equation (1) where the Maxwell distribution is expressed as a differential equation, the number of gas molecules is denoted by N. This N is, for gas molecules contained in a volume, very large. For example, the-number of hydrogen molecules contained in a cubic centimeter at standard temperature and pressure (STP) is about 5.36 x lO^{19} molecules/cm^3· This is a large "sample size" compared to the "large" samples sizes used in the medical, biological or social sciences. However, some reasonable estimate of a sample size could be required for measurements of the velocity of human head motion. Obtaining such an estimate is addressed next.

Suppose an objective of a study was to determine if the measurements made were done on entities drawn from Gauss distribution or from a Maxwell distribution. The determination could be done by comparing the observed measures of skewness and kurtosis with the theoretical values of these statistics for the Gauss distribution. Let the first null hypothesis be:

$$H_0 : \beta_1(G) - \beta_{1,2} = 0, \qquad (44)$$

where $\beta_1(G) = 0$ for the Gauss distribution, $\beta_1 = 0.2359$ for the Maxwell distribution, and $\hat{\beta}_1$ the observed value. To test this hypothesis, the variance of $\beta_1(G)$ is needed. The variance of $\beta_1(G)$ [and $\beta_2(G)$] is a function of the sample size, n only (Snedecor and Cochran, 1956). If a t-test is to be used and the level-of significance, alpha, is set equal to $p = 0.05$ for a one-tailed or one-sided test, then for a t-value of 1.64 and using the formula from Snedecor and Cochran, a sample size of # 285 # n # 295 is found. These values were found by numerical methods.

To test the null hypothesis in the case of β_2 - - kurtosis - - the null hypothesis takes the form:

$$H_o: \beta_2(G) - \beta_2 = 0, \qquad (45)$$

where $\beta_2(G) = 3$, $\beta_2 = 3.1082$ for the Maxwell distribution, and β_2, is the observed value. Using the same method cited above, the sample size needed to test this null hypothesis is $5500 \leq n \leq 5550$.

These relatively large samples are, in the main, due to the fact ~hat very small differences are to be detected. In the case of β_1, the difference between the Gauss and Maxwell distributions is 0.2359. In the case of β_2, the difference to be detected is 0.1082 between the theorectical values for the Gauss and Maxwell distributions. Furthermore, the variance of both β_1 and β_2 are functions of the higher moments of the Gauss distribution, *i.e.*, functions of the fifth through eight moments. This fact begins to get the experimenter into a never-never land of statistical machinatiops. The point is, nonetheless, that relatively huge sample sizes (measurements) are needed in an attempt to determine which of these two distributions is the one from which the sample of measurements was drawn.

SUMMARY

The purpose of Appendix B is to give the derivation of the moments and measures of skewness, β_1, and kurtosis, β_2, of the Maxwell probability distribution function (p.d.f.). These are needed in connection with the development of a stochastic model of helicopter pilots' head motion during flight while engaged in searching for another helicopter.

The Maxwell p.d.f, is given with a pr6cis of its history. The first four central moments are derived as well as the measures of skewness and kurtosis. These are derived for both E. Parzen's (Parzen, 1960) and C. P. Tsokos' (1972) formulation of the Maxwell p.d.f. The expected values of the "raw" moments and moments around 2 are displayed in Table B-1. The formulae for β_1 and β_2 were used to obtain numerical estimates for them. The β_1 estimate is 0.235898 and the β_2 estimate is 3.10816.

The method of moments is used to obtain estimators for the mean and variance of the Maxwell p.d.f. The estimator for the sample mean, 6, is equal to $2\theta / \sqrt{\pi}$ where θ is the parameter in the Maxwell p.d.f. The estimator for the sample variance, σ^2, is equal to $\theta^2(3 / 2 - 4 / \pi)$. These equations can be used to obtain a sample estimate of θ given 6 and σ^2 values. These estimators were needed in conjunction with the stochastic modeling of aviator head motion. The literature extant on the Maxwell p.d.f, did not provide estimators of the parameter θ (or of α in Tsokos' notation where $\alpha = \sqrt{\pi}2 / \theta$).

The Maxwell p.d.f, is a member of the family exponential p.d.f. The Gauss (Normal) p.d.f, is also a member of that family. The Maxwell and the Gauss p.d.f, are related to each other via consideration of Brownian Motion (BMO). However, the Gauss distribution has two parameters while the Maxwell distribution has one parameter. A graph of the Maxwell distribution (displayed in Figure B-l) with the Gauss distribution superimposed shows that the Maxwell distribution is skewed with a long tail extending in tile right-hand direction. The Maxwell distribution is "more peaked" than is the Gauss one and it's density is asymmetric.

For small samples sizes of velocity, a sample drawn from a Maxwell distribution would be nearly indistinguishable from a sample drawn from a Gauss distribution. Large sample sizes would be needed to test whether or not the underlying process was a Maxwell or a Gaussian distribution if the measures of skewness and kurtosis are used to distinguish between the two.

If the assumption is made that the underlying distribution for a process is the Maxwell p.d.f., then the data values could be transformed using g(m) = 1.8311 ln(x) so as to stabilize the variance(s) for a particular statistical analysis.

REFERENCES

Bartlett, M. S. 1947. The Use of Transformations. *Biometrics* 3:39-52.

Box, G. E. P. 1984. Personal communication.

Doob, J. L. 1942. The Brownian movement and stochastic equations. *Annals of Math.:* 43(2):351-369.

Durrett, R. 1984. Brownian Motion and Martingales in Analysis. Belmont, CA: Wadsworth Advanced Books & Software.

Einstein, A. 1926. Investigations on the Theory of the Browninan Motion (R. Furth, ed and translated by A. D. Cowper}. NY: Dover Publications Inc. (Dr. Einstein wrote the first paper in the above text in 1905.)

Everitt, B. S. and Hand, D. J. 1981. Finite Mixture Distributions. NY: Chapman and Hall.

Feller, W. 1971. An Introduction to Probability Theory and Its Applications: Vol. II. John Wiley and Sons, Inc.

Forsythe, A. B. 1984. Personal communication.

Freund, J. E. 1971. Mathematical Statistics. Englewood Cliffs, NJ: Prentice-Hall, Inc.

Hasting, N. A. J. and Peacock, J. G. 1975. Statistical Distributions. NY: John Wiley and Sons.

Johnson, N. L. and Kotz, S. 1970. Continuous Univariate Distributions-l. Boston, MA: Houghton Mifflin Co.

Johnson, N. L. and Kotz, S. 1972. Distributions in Statistics: Continuous Multivariate Distributions. NY: John Wiley & Sons, Inc.

Kendall, M. G. and Stuart, A. 1966. Tile Advanced Theory of Statistics, Vol. 3. London, England: Charles Griffing and Company LTD.

Kendall, M. G. and Stuart, A. 1963. The Advanced Theory o-ff Statistics: Vol. I. NY: Hafner Publishing Company.

Marshall, E. A. 1984. Dynamical equations for the stride swing in human walking. In Mathematics in Medicine and Biomechanics. Roach, G. F. (ed.) Cheshire, England: Shira Publishing Co.

Menzel, D. H. (ed). 1960. Fundamental Formulas of Physics: Volume One. NY- Dover Publications, Inc.

Morgan, B. J. T. 1984. Elements of Simulation. London, England: Chapman and Hall.

Niven, W. D. (ed). 1965. The Scientific Papers of James Clerk Maxwell. NY: Dover Publications, Inc.

Parzen, E. 1960. Modern Probability Theory and Its Applications. NY:John Wiley & Sons, Inc.

Sears, F. W. and Zemansky, M. W. 1963. University Physics, Part 1.Reading, MA: Addison-Wesley Publishing Co.

Snedecor, G. W. and Cochran, W. G. 1956. Statistical Methods. Ames, IA: The Iowa State College Press.

Tsokos, C. P. 1972. Probability Distributions: An Introduction to Probability Theory with Applications. Belmont, CF: Duxbury PresT.

Wang, M. C. and Uhlenbeck, G. E. 1945. On the Theory of the Brownian MotionII. *Reviews of Modern Physics:* 17:323-342.

Wax, M. (ed). 1954. Selected Papers on Noise and Stochastic Processes: NY: Dover Publications, Inc.

Wilks, S. S. 1962. Mathematical Statistics. NY: John Wiley and Sons, Inc.

Appendix C

List of Manufacturers

Honeywell, Inc.
1625 Zarthan Avenue, South
P.O. Box 38
Minneapolis, MN 55440